

**PAN-AFRICAN UNIVERSITY**  
**INSTITUTE FOR WATER AND ENERGY SCIENCES**  
**(including CLIMATE CHANGE)**

# **Master Dissertation**

Submitted in partial fulfillment of the requirements for the Master degree in  
**CLIMATE CHANGE ENGINEERING**

Presented by

***Hadjer ADJADJ***

**TITLE: Analysis of Flood Risk and Strategic Management to Address Its Adverse  
Impacts: A Case Study of the Boudouaou Basin, Algiers, Algeria.**

*Defended on 20/04/2025 Before the Following Committee:*

<b>Chair</b>	Tayeb Boulmaiz	Prof	University of Ghardaia, Algeria
<b>Supervisor</b>	Sameh Kantoush	Prof	University of Tokyo, Japan
<b>Co-supervisor</b>	Chérifa Abdelbaki	Prof	University of Tlemcen, Algeria
<b>External Examiner</b>	Serigne Faya	Prof	Affiliation (Institution only)
<b>Internal Examiner</b>	Bouanani Abderrezak	Prof	University of Tlemcen, Algeria

# APPROVAL SHEET

## **Analysis of Flood Risk and Strategic Management to address its adverse impacts: A Case Study of the Boudouaou Basin, Algiers, Algeria.**

A thesis submitted to the Pan African University Institute of Water and Energy Sciences (including Climate Change) in partial fulfillment of the requirements for the degree of Master of Science in Climate Change (Engineering option).

By

Hadjer ADJADJ

Supervisor: Prof. Sameh Kantoush

03/04/2025

Co-supervisor: Prof. Chérifa Abdelbaki

03/04/2025

April 2025

Tlemcen, Algeria

## **DEDICATION**

I dedicate this thesis to my beloved family and friends, whose unwavering love and support have made this achievement possible.

## **STATEMENT OF THE AUTHOR**

I, Hadjer ADJADJ, declare that this thesis is my work. I have followed all ethical principles of scholarship in the preparation, data collection, data analysis, and completion of this thesis. I have given all scholarly matter recognition through accurate citations and references. I affirm that I have cited and referenced all sources used in this document.

I submit this document in partial fulfillment of the requirement for a degree from Pan African University. This document is available from the PAU Library to borrowers under the rules of the library. I declare that I have not submitted this document to any other institution for the award of an academic degree, diploma, or certificate.

## ACKNOWLEDGMENT

I am profoundly thankful to my mentors, Dr. Sameh Kantoush and Dr. Chérifa Abdelbaki, for the extensive expertise and assistance they have provided, enabling me to successfully accomplish this thesis.

A special acknowledgment and heartfelt appreciation are directed towards Eng. Hadir Abdelmoneim for her remarkable assistance, altruism, invaluable guidance, feedback, and support throughout this research.

Thanks also go to Yacine Abdelbaset Berrezel for his valuable support, guidance, and feedback in the due course of the accomplishment of this thesis.

I wish to extend my sincere thanks to Mr. BENMOUFFOK HOUCINE and the staff of the National Agency for Hydraulic Resources (ANRH) in Algiers for welcoming me and providing an enriching internship experience that greatly benefited this research.

My acknowledgment and deepest gratitude go to the University of Sharjah, particularly the Department of Civil and Environmental Engineering, for hosting me during my internship period. A special thank you to Professor Tarek Merabtene for his invaluable supervision, guidance, and support throughout my stay.

I am deeply grateful to my entire family, my friends and to all those who contributed, directly or indirectly, to the successful completion of this thesis.

## ABBREVIATION AND ACRONYMS

AHP	Analytic Hierarchy Process
RRI	Rainfall-Runoff-Inundation
IPCC	Intergovernmental Panel on Climate Change
CUI	Command User Interface
GUI	Graphical User Interface
GIS	Geographic Information System
MCDM	multi-criteria Decision-Making
LU/LC	Land use/Land cover
USGS	United States Geological Survey
ICHARM	International Centre for Water Hazard and Risk Management
DEM	Digital Elevation Model
SDG	Sustainable Development Goal
TWI	Topographic Wetness Index
NSE	Nash-Sutcliffe model efficiency coefficient
ANBT	National Agency for Dams and Transfers
ANRH	National Agency for Water Resources
ORD	Oxford Reference Dictionary
WHO	World Health Organization
UNESCO	United Nations Educational, Scientific and Cultural Organization
FLM	Fuzzy Logic Modelling
ANN	Artificial Neural Networks
HEC-RAS	Hydrologic Engineering Center's River Analysis System
HEC-HMS	Hydrologic Engineering Center's Hydrologic Modeling System

# TABLE OF CONTENTS

APPROVAL SHEET .....	i
DEDICATION .....	ii
STATEMENT OF THE AUTHOR .....	iii
ACKNOWLEDGMENT.....	iv
ABBREVIATION AND ACRONYMS .....	v
ABSTRACT .....	xi
CHAPTER ONE: INTRODUCTION .....	1
1.1 Background.....	1
1.2 Problem Statement .....	2
1.3 Objectives.....	4
1.3.1 Main Objective .....	4
1.3.2 Specific objectives.....	4
1.4 Research questions .....	4
1.5 Justification of the study.....	4
1.6 Scope of the study .....	5
1.6.1 Geographical scope .....	5
1.6.2 Content scope.....	5
1.7 Thesis Layout.....	5
CHAPTER TWO: LITERATURE REVIEW.....	7
2.1 Introduction .....	7
2.2 Flood definition.....	7
2.3 Previous work in Algeria .....	8
2.4 Flood hazard Assessment.....	9
2.5 Flood vulnerability assessment .....	10
2.6 Flood risk assessment.....	11
2.7 Analytical hierarchy process (AHP) model.....	12

<b>2.8</b>	<b>Rainfall-Runoff Models</b> .....	13
<b>CHAPTER THREE: METHODOLOGY</b> .....		16
<b>3.1</b>	<b>Definition</b> .....	16
<b>3.2</b>	<b>Study area</b> .....	16
<b>3.2.1</b>	<b>Geographical Location</b> .....	16
<b>3.2.2</b>	<b>Topographical and hydrological characteristics</b> .....	17
<b>3.2.3</b>	<b>Geometric characteristics</b> .....	17
<b>3.2.3.1</b>	<b>Area and perimeter of the basin</b> .....	17
<b>3.2.3.2</b>	<b>Shape characteristics</b> .....	17
<b>3.2.4</b>	<b>Relief characteristics</b> .....	18
<b>3.2.4.1</b>	<b>Basin elevation</b> .....	18
<b>3.2.4.2</b>	<b>Slope</b> .....	20
<b>3.3</b>	<b>Data collection</b> .....	21
<b>3.3.1</b>	<b>Rainfall data</b> .....	22
<b>3.3.2</b>	<b>Discharge data</b> .....	23
<b>3.3.3</b>	<b>Remote Sensing Data</b> .....	23
<b>3.3.3.1</b>	<b>Digital Elevation Model (DEM)</b> .....	23
<b>3.3.3.2</b>	<b>Land use/cover</b> .....	24
<b>3.4</b>	<b>Software required for the processing of data</b> .....	25
<b>3.4.1</b>	<b>ArcGIS</b> .....	25
<b>3.4.2</b>	<b>Rainfall-Runoff Inundation Model</b> .....	25
<b>3.4.2.1</b>	<b>RRI Model Input</b> .....	26
<b>3.4.2.2</b>	<b>Model simulation</b> .....	29
<b>3.4.2.3</b>	<b>Model calibration and validation</b> .....	30
<b>3.5</b>	<b>Flood Hazard mapping</b> .....	31
<b>3.6</b>	<b>Flood Vulnerability mapping</b> .....	31
<b>3.7</b>	<b>Analytical Hierarchical Process (AHP) method</b> .....	32

3.7.1 Pairwise comparison matrix .....	32
3.7.2. Normalized pairwise comparison matrix. ....	33
3.7.3. Consistency .....	34
3.8 Flood Risk Map .....	34
3.9 Proposed mitigation strategies .....	35
<b>CHAPTER FOUR: RESULTS AND DISCUSSIONS.....</b>	<b>36</b>
<b>Part 01: Flood vulnerability assessment using AHP method.....</b>	<b>36</b>
4.1.1 Introduction.....	36
4.1.2 Flood vulnerability assessment.....	37
4.1.2.1 Defined the criteria: .....	37
4.1.2.2 AHP weighting factors .....	39
4.1.3 Results & discussion:.....	42
<b>Part 02: Flood Hazard Mapping using the RRI Model .....</b>	<b>46</b>
4.2.1 Introduction.....	46
4.2.2 Model Calibration and Validation.....	46
4.2.3 Simulation Scenarios and Setup.....	46
4.2.3.1 Scenarios 1: without the Dam and with the dam .....	47
4.2.3.2 Comparative Analysis of Scenarios .....	48
<b>Part 03: Flood risk mapping .....</b>	<b>51</b>
4.3.1 Introduction.....	51
4.3.2 Flood Risk Maps and Interpretation .....	51
A. Actual rainfall event scenario.....	51
B. Increased Rainfall Conditions scenario (20%, 60%, 100%) .....	52
4.3.3 Proposed Flood Risk Management Solutions .....	54
<b>CHAPTER FIVE: CONCLUSION .....</b>	<b>56</b>
<b>6.1 Conclusion.....</b>	<b>56</b>
<b>CHAPTER SIX: REFERENCES .....</b>	<b>57</b>

## LIST OF TABLES

<b>Table 1:</b> Comparison of the basic structure for rainfall-runoff models (Sitterson et al., 2018; Jehanzaib et al., 2022). .....	13
<b>Table 2:</b> Classification of relief according to (Ig) given by ORSTOM (Source: Msatef et al., 2018). .....	20
<b>Table 3:</b> Physical characteristics of Boudouaou Watershed. ....	21
<b>Table 4:</b> Data Type and source. ....	22
<b>Table 5:</b> Rainfall stations in the Boudouaou basin. ....	23
<b>Table 6:</b> Discharge stations in the Boudouaou basin. ....	23
<b>Table 7:</b> Scores for the importance of variable. ....	32
<b>Table 8:</b> The value of Random Consistency Index. ....	34
<b>Table 9:</b> Pairwise comparison matrix. ....	40
<b>Table 10:</b> Normalized pair-wise comparison and weight values of flood attribute. ....	41
<b>Table 11:</b> The consistency ratio. ....	41
<b>Table 12:</b> Flood Vulnerability Factors and Rating Scale. ....	43

## LIST OF FIGURES

<b>Figure 1:</b> Map of disastrous floods in Algeria (1965–2013) (source: Boutaghane et al., 2021). .....	2
<b>Figure 2:</b> Flooding in Kharouba City (Source: provided by local residents). .....	3
<b>Figure 3:</b> Bridge 2 (Br-2) during the flood event (Source: Otmane et al., 2024). .....	4
<b>Figure 4:</b> Location of the study area. ....	16
<b>Figure 5:</b> Elevation distribution map of the Wadi Khemis Basin. ....	19
<b>Figure 6:</b> Elevation distribution map of the Wadi Khemis Basin. ....	19
<b>Figure 7:</b> Slope distribution map of the Wadi Boudouaou Basin. ....	21
<b>Figure 8:</b> Land use/cover distribution within the Wadi Boudouaou Basin in 2023 derived from the 2023 Esri Sentinel-2 Land Cover. ....	24
<b>Figure 9:</b> Schematic diagram of the rainfall–runoff–inundation (RRI) model. ....	25
<b>Figure 10:</b> Topographical characteristics of the Nan River Basin. (a) Topography; (b) Flow direction; and (c) Flow accumulation. ....	28
<b>Figure 11:</b> Percentage of land use/land cover types within Wadi Boudouaou watershed. ....	29
<b>Figure 12:</b> Flowchart of Flood Vulnerability Assessment Using Analytical Hierarchy Process (AHP). ....	36
<b>Figure 13:</b> Factors classification. ....	45
<b>Figure 14:</b> Flood vulnerability map. ....	45
<b>Figure 15:</b> Hazard Maps Under Increased Rainfall Scenarios (Without Dam: +20%, +60%, +100%). ....	50
<b>Figure 16:</b> Flood Risk map. ....	52
<b>Figure 17:</b> Flood Risk Maps Under Increased Rainfall Conditions (20%, 60%, 100%). ....	54

## ABSTRACT

Flooding is a significant and worsening challenge for many human societies, with increasing severity driven by climate change and land use pressures. This natural hazard constitutes one of the world's worst natural disasters, causing about a third of all significant human, material, and economic losses, highlighting the urgent need for effective flood risk management strategies. This study assessed the flood risk in the Wadi Boudouaou basin using an integrated approach that combines the Analytical Hierarchy Process method and the Rainfall Runoff Inundation Model to identify high-risk areas. The AHP method was applied to develop a flood vulnerability map based on seven key criteria: elevation, slope, rainfall, land use/land cover, drainage density, topographic wetness index and distance from river to provide a spatial understanding of areas with varying susceptibility to flood impacts. The RRI model was used to simulate flood hazard under two major scenarios: with and without the presence of the Keddara Dam. However, the presence of the dam produced negligible differences in flood hazard patterns. Furthermore, four rainfall conditions were tested: the actual recorded event, and hypothetical increases of 20%, 60%, and 100% to simulate the effects of future climate change. Analysis of the risk map illustrates that the areas situated in proximity to the main Boudouaou Wadi exhibit very high to high risk to flooding incidents compared to other parts of the watershed. Additionally, the results showed that flood risk increases significantly with higher rainfall intensities, particularly along main river channels and low-lying floodplains, emphasizing the pressing need for proactive flood risk management measures. The findings will provide policymakers, urban planners, and disaster management authorities with actionable strategies to reduce flood risk and enhance long-term resilience in the Wadi Boudouaou Basin.

**Keywords:** Wadi Boudouaou basin, Flood risk, Flood hazard, Vulnerability mapping, AHP method, RRI model, GIS.

**1**

---

## **Introduction**

# CHAPTER ONE: INTRODUCTION

## 1.1 Background

In recent decades, the management of water resources has become a critical global concern due to the increasing frequency and intensity of extreme hydrometeorological events driven by climate change. Rising temperatures and changes in precipitation patterns have intensified both droughts and floods, resulting in significant socio-economic and environmental consequences (Kundzewicz et al., 2019). Among these, floods represent one of the most destructive natural hazards, causing widespread damage to infrastructure, loss of life, and economic disruptions (Merz et al., 2021).

Floods can occur due to various factors, including intense or prolonged rainfall, poor drainage infrastructure, and land-use changes that reduce natural water retention capacities (Hassan et al., 2022; Zhang et al., 2022). Urbanization exacerbates the risk of flooding by increasing impervious surfaces, which accelerate surface runoff and reduce infiltration. This is particularly concerning in rapidly developing regions where urban expansion outpaces the implementation of effective flood control measures (Douglas et al., 2008).

Algeria, like many Mediterranean countries, has been increasingly affected by extreme flood events, primarily due to its climatic variability and rapid urbanization (Zekouda et al., 2020). The country experiences heavy seasonal rainfall, which, when combined with inadequate drainage systems and unplanned urban sprawl, leads to severe flooding, particularly in densely populated areas (Abdrabo et al., 2021). Notable flood disasters in Algeria include the devastating floods in Bab El Oued (2001), Ghardaïa (2008), and Algiers (2018), all of which caused significant casualties and economic losses (Taib, 2024)

The Boudouaou Basin, located in the Algiers region, is particularly vulnerable to flood hazards due to its geographical and hydrological characteristics. The basin's proximity to urbanized areas, combined with rapid land-use changes and insufficient flood mitigation strategies, has increased the likelihood of recurrent flooding. Heavy rainfall events frequently lead to flash floods, overwhelming drainage systems and causing damage to residential, commercial, and agricultural areas. Additionally, sediment transport and riverbed modifications contribute to further disruptions, reducing the basin's capacity to manage floodwaters effectively.

Despite the availability of various flood risk assessment tools, a major challenge remains in accurately identifying high-risk areas and vulnerable infrastructure in the Boudouaou Basin. Effective flood risk management requires an integrated approach that combines hydrological

modeling, hazard assessment, and vulnerability analysis to capture the complexity of flood dynamics. In this context, flood hazard and vulnerability maps play a crucial role in developing comprehensive flood risk maps for different return periods, allowing for a more precise assessment of exposure and potential damage. This study employs the Rainfall-Runoff-Inundation (RRI) model alongside the Analytic Hierarchy Process (AHP) method to enhance flood risk mapping, providing valuable insights into areas at heightened risk of flooding.

Building on these assessments, the study aims to develop strategic mitigation measures and preparedness actions to reduce flood risks in the Boudouaou Basin. By analyzing flood-prone zones and critical infrastructure exposure, the research will support risk-informed decision-making, and the development of adaptive strategies tailored to the region’s hydrological and socio-economic conditions. The findings will contribute to improving flood resilience through early warning systems, land-use planning, and targeted infrastructure enhancements, ensuring that communities are better equipped to withstand future flood events.

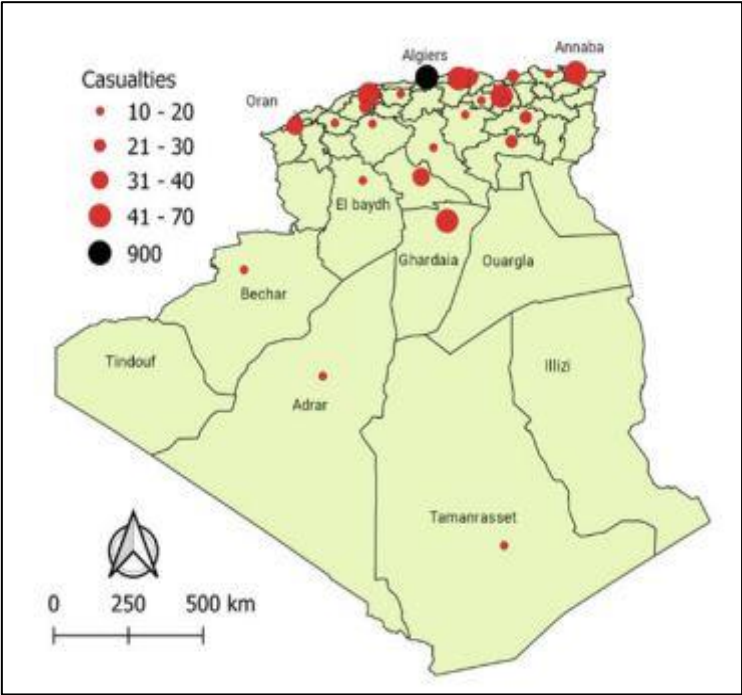


**Figure 1:** Map of disastrous floods in Algeria (1965–2013) (source: Boutaghane et al., 2021).

**1.2 Problem Statement**

Flooding is one of the most frequent and destructive natural hazards, with increasing intensity due to climate change, rapid urbanization, and unregulated land use. Algiers, like many urban centers, faces escalating flood risks, driven by population growth and infrastructure expansion

into flood-prone areas. Between 1987 and 2008, the urban population of Algiers grew from 1.6 million to over 4 million and was projected to reach 7 million by 2015 (ONS, 2013; Population Data, 2020). Over the same period, the urbanized area tripled, significantly altering the region’s natural drainage systems and increasing flood susceptibility (Ziadi et al., 2023).

The Boudouaou Basin, a key watershed in Algiers, has experienced frequent and severe floods, causing extensive damage to infrastructure, economic activities, and communities. According to the Civil Protection Services census, 174 flood events were recorded between 1946 and 2021, with several causing significant losses (Ziadi et al., 2023). Contributing factors include climate variability, increasing urban pressure on floodplains, and inadequate flood management strategies. Despite these challenges, limited research has been conducted on flood risk assessment in the Boudouaou Basin leaving an essential gap in understanding flood hazards and vulnerabilities.

To address this gap, this study will assess flood risk in the Boudouaou Basin by identifying high-risk areas using flood hazard and vulnerability mapping. The research will integrate the Rainfall-Runoff-Inundation (RRI) model and the Analytic Hierarchy Process (AHP) method to develop flood risk maps for different scenarios. Furthermore, it will propose targeted flood mitigation strategies, such as improving drainage systems, implementing retention ponds, and promoting green infrastructure, to enhance resilience and support informed decision-making in flood management.



**Figure 2:** Flooding in Kharouba City (Source: provided by local residents).



**Figure 3:** Bridge 2 (Br-2) during the flood event (Source: Otmane et al., 2024).

### **1.3 Objectives**

#### **1.3.1 Main Objective**

The main objective of this work is to develop a flood risk map of the Boudouaou Wadi watershed and suggest possible mitigation measures.

#### **1.3.2 Specific objectives**

To apply a Rainfall-Runoff Inundation (RRI) model to develop flood hazard maps for different scenarios, and Flood vulnerability map using Analytical Hierarchy Process (AHP) method.

To develop a flood risk maps within Boudouaou watershed.

Suggest appropriate mitigation measures and actions to reduce the risk in Boudouaou watershed.

### **1.4 Research questions**

What are the major factors contributing to flooding in the Boudouaou watershed?

What are the areas most affected by floods in the Boudouaou watershed?

What are the possible flood mitigation and adaptation strategies for reducing flood risk in Boudouaou watershed?

### **1.5 Justification of the study**

Floods are among the most frequent and destructive natural hazards, posing significant threats to infrastructure, livelihoods, and ecosystems (Aldardasawi & Eren, 2021). In the Boudouaou

Basin, Algiers, rapid urbanization and climate variability have intensified flood risks, emphasizing the need for comprehensive flood risk assessment and mitigation strategies.

This study provides critical insights by integrating vulnerability mapping using multi-criteria decision analysis (AHP) with flood hazard modeling through the RRI model to identify high-risk areas and critical infrastructure. Addressing this knowledge gap enhances flood preparedness, supports data-driven urban planning, and strengthens disaster risk management.

Moreover, this research aligns with Sustainable Development Goal (SDG) 13: Climate Action, which calls for urgent adaptation measures to mitigate climate-related risks. By advancing flood risk assessment and mitigation, this study contributes to climate resilience, informs sustainable land-use planning, and supports the development of early warning systems and flood protection measures.

Ultimately, the findings will provide policymakers, urban planners, and disaster management authorities with actionable strategies to reduce flood risk and enhance long-term resilience in the Boudouaou Basin and beyond.

## **1.6 Scope of the study**

### **1.6.1 Geographical scope**

The geographical scope of this research focuses on the Boudouaou watershed, which is a sub-basin of the large Algiers coastal basin (02a), located in the northern part of Algeria with a total area of 149.98 km<sup>2</sup>.

### **1.6.2 Content scope**

The study focused on applying the Rainfall-Runoff-Inundation (RRI) model to simulate and map flood hazards and employing the Analytical Hierarchy Process (AHP) for detailed vulnerability assessment based on clearly defined criteria. The integration of these hazard and vulnerability assessments provides flood risk maps within the Boudouaou watershed and identifies flood risk zones. Finally, the study proposes targeted flood risk reduction strategies to reduce the risk in the Boudouaou watershed.

## **1.7 Thesis Layout**

This thesis is divided into six chapters.

**Chapter 1 - Introduction:** This chapter presents an Introduction, the background context for the research topic, defines the problem statement, outlines the study objectives and research questions, explains the significance of the study.

**Chapter 2 - Literature Review:** A Literature Review organized into eight sections: (1) Introduction, (2) flood definition, (3) Previous work in Algeria, (4) Flood hazard Assessment, (5) Flood vulnerability assessment, (6) Flood Risk Assessment, (7) Analytical hierarchy process (AHP) model, (8) Rainfall-Runoff Models will be discussed in this chapter.

**Chapter 3 - Methodology:** This will delve into a detailed exploration of the watershed geographical extent, study Area description, data collection, and software used.

**Chapter 4 - Results and discussion:** This section will present the results of the research and discussion.

**Chapter 5 - Conclusion and Recommendation:** Conclusion and Recommendations will be discussed in this chapter.

**Chapter 6 - References.**

---

**LITERATURE REVIEW**

## **CHAPTER TWO: LITERATURE REVIEW**

### **2.1 Introduction**

Floods are among the most harmful natural disasters, and population growth, along with rapid urbanization, raises flood risks in many areas globally. Almost every nation experiences floods, but the damage is greatest in developing countries. Flood risk management is therefore crucial in those areas to assess the potential hazards, mitigate the impacts, and build resilience to future events. This literature review aims to provide a comprehensive overview of flood research in the context of the Boudouaou Basin in Algeria to establish a foundation for the study. The review covers definitions, types, previous research on flood risk assessment and vulnerability, the Analytical Hierarchy Process (AHP) method, and the Rainfall Runoff Inundation Model (RRI).

### **2.2 Flood definition**

Floods are common in all parts of the world, and their characteristics and intensity vary from region to region (Tariq, 2012). The etymology of the word flood goes back to the Old English word 'flod' akin to the German word 'flut' and the Dutch word 'vloed' which stands for inflow and float of water (Glago, 2021). In the glossary of the Oxford Reference Dictionary (ORD), a flood is defined as an overflow or influx of water that exceeds its typical boundaries.

Flooding typically occurs when the volume of water within a water body, such as a river or lake, exceeds its total capacity, causing some of the water to flow outside the water body's typical boundaries (Glago, 2021). Furthermore, floods are described as "the overflowing of the normal boundaries of a stream or other water bodies or the accumulation of water in areas that are not typically submerged" in the IPCC SREX report's glossary (Kundzewicz et al., 2013). Moreover, the article by Chan et al. (2022) defines flooding as an upward condition of water levels reservoirs, streams, canals, and coastal regions that leads to widespread damage, disrupts daily life, and increases vulnerability in various aspects such as social, physical, economic, and environmental factors. In addition, there are certain human activities that lead to aggravation of flood occurrence frequency and its consequences (Tariq, 2012).

According to WHO (2019), floods, the most common natural disaster, happen when an overflow of water submerges land that is typically dry. They are often triggered by heavy rainfall, a storm surge from a tropical cyclone, rapid snowmelt, or a tsunami in coastal areas. Floods can be

categorized into three common types: flash floods, river floods, and coastal floods. However, flash floods are characterized by their short duration, rapid and intense rainfall that raise water heights with limited time for response (Maqtan et al., 2022; Helmi & Zohny, 2020). River floods occur when a river overflows its banks. This typically happens when prolonged rainfall, storm surges, or seasonal snowmelt drive a river to exceed capacity (Merz et al., 2021). Coastal floods, on the other hand, are caused by sea level rise or storm surges associated with tropical cyclones and tsunamis (Koks et al., 2022).

### **2.3 Previous work in Algeria**

The flood research is the first step toward a better understanding of the phenomenon for improving management. The number of research studies documenting Algeria's floods has increased recently (Boutaghane et al., 2021). A study conducted by Astite et al. (2015) in Oued El Harrach (north of Algeria) presents the management of flood risk through the use of cartography of flood hazard using HECRAS and ArcGIS. It is highlighted that the use of flood zones as habitats for people was the main causes of losses in this area. Moreover, many researchers across Algeria have integrated the HECRAS with geospatial data through a geographic information system (GIS) to create flood risk maps, such as those conducted by Boulaghmen et al. (2018) in Ghardaia, Abdessamed & Abderrazak (2019) in Ain Sefra, and Madi et al. (2020) in Bechar.

Over the last few years, studies using the Analytical Hierarchy Process (AHP) have exploded in Algeria, while there have been very few studies on the RRI (Rainfall Runoff Inundation) model for assessing and mapping flood hazard. Belazreg et al. (2023) studied the El-Ham watershed located in the Hodna basin, applying AHP techniques in conjunction with Geographic Information Systems (GIS) to prepare updated flood risk hazard maps. The study identified six key criteria influencing flood hazards: slope, drainage density, annual maximum daily precipitation, elevation, land use/cover, and soil type. The study showed the areas in the northeastern, northwestern, and central regions of the study site have a high potential for flooding, which implies that the chosen criteria were adequate for producing reliable flood risk maps. The authors also noted that incorporating additional parameters through hydrological models like RRI could provide more detailed insights. In another study, Rebouh et al. (2024) applied AHP, GIS, remote sensing, and Google Earth Engine to measure flood vulnerability in Ain Smara and the regions around Constantine. The methodology as developed was able to capture areas prone to floods, which indicates the effectiveness of using different geospatial

data sources and analytical techniques in creating comprehensive mapping of flood susceptibility. The study considered several key criteria influencing flood vulnerability, such as elevation, topographic wetness index, slope, precipitation, land cover, and land use. The Topographic Wetness Index was identified as the most significant criterion. A recent study by Afra et al. (2025) in Algeria adopted the Rainfall–Runoff–Inundation Model to address flood risk in the Makkera basin. The RRI model demonstrated a strong performance and highlights its utility for flood risk assessment in arid and semi-arid regions.

## **2.4 Flood hazard Assessment**

The objective of flood hazard assessment is to understand the likelihood that a flood of a specific intensity will occur over a defined period in specific locations (World Bank, 2016). Assessing flood hazards is a complex task that involves the use of multiple methods. The selection of the appropriate method depends on the needs of the study area and the availability of data (Manandhar, 2023b). By estimating this probability over periods of years to decades, hazard assessments contribute to supporting risk management activities (World Bank, 2016).

In 2016, Vojtek and Vojteková conducted a study in Slovakia focusing on assessing flood risks at a local scale. This study highlights the increased use of GIS and remote sensing to develop versatile hazard maps for risk and determination of flood risk, which represent a combination of the model area's vulnerability and flood hazard. Nevertheless, the study employed a 1D hydraulic model (HEC-RAS), which may not adequately represent the intricacies of unsteady flows or interactions in regions with complex terrain, despite being useful for steady-flow analysis. The study conducted by Kvočka et al. (2016) compared two types of flood hazard assessment, empirically Derived Methods which use simplified equations to assess flood threats like those by Ramsbottom et al. (2006), and Physically Based and Experimentally Calibrated Methods which take into consideration all of the physical forces acting on a human body in floodwaters, account for rapid fluctuations in the flow regime, typical of extreme flood events, and enable a swift assessment of flood hazard risk in a short period of time, such as those proposed by Xia et al. (2014). The 2007 Železniki flash flood and the 2010 Kostanjevica na Krki river flood served as case studies to show that mechanics-based approaches are more appropriate for extreme events. However, the physical based method is limited by its tendency to average flow regime values, such as the population's ability to navigate through floodwaters and the psychological and demographic factors that have a substantial impact on human stability in floodwaters, such as age, fear, or physical disabilities, which may not fully represent

the actual conditions of the general population. Researchers have increasingly employed multi-criteria decision-making methods, especially the Analytical Hierarchy Process (AHP) supported by Geographic Information Systems (GIS), and highlighted its effectiveness to comprehensively assess flood hazard, such as Seejata et al. (2018), Khoeun et al. (2022), Hagos et al. (2022), Ghosh (2023), Ahmed et al. (2023), and Aichi et al. (2024). The study by Sayama et al. (2012) explores the combined use of the Analytical Hierarchy Process (AHP) for the assessment of flood hazard and rainfall-runoff inundation (RRI) model, which simulates flood inundation and rainfall runoff concurrently.

## **2.5 Flood vulnerability assessment**

The primary objective of flood vulnerability assessment is providing a better understanding of flood risk management by identifying vulnerable areas, taking proactive steps to reduce the impacts of flooding, building resilience to future events, and developing strategies to mitigate the damage (Schwarz & Kuleshov, 2022; Chan et al., 2022; Nasiri et al., 2016).

According to Chan et al. (2022), different methods were employed to assess the susceptibility, such as indicator-based method, modelling methods through geographic information systems, the vulnerability curve method, the mapping method, the analytical hierarchy process, and the disaster loss data method. Noteworthy studies, including those conducted by Mondal et al. (2019), An et al. (2022) in Vietnam, and Ayenew & Kebede (2023) in Ethiopia, illustrate the efficacy of using Geographic Information Systems (GIS) and remote sensing techniques in assessing flood vulnerability. Hanan et al. (2022) have emphasized the vital role that GIS plays by providing timely, cost effective, and accurate information that can be utilized for urban planning and disaster mitigation to reduce the risk of life and property losses. However, several studies highlight the limitations of conventional flood vulnerability assessments, which often focus on physical factors and neglect social and economic aspects that are crucial in comprehensive flood risk assessment (Chan et al., 2022). In addition, another study in Lajeado and Estrela in the southernmost state of Brazil highlights the strengths and adaptability of MCDM methods in flood vulnerability assessments (De Brito et al., 2018). For example, the Analytical hierarchy process was used by Vignesh et al. (2020) in Kanyakumari District, India, to evaluate flood-prone zones. The study employed the AHP technique to assign weights to ten critical parameters based on their importance in contributing to flood risk, including rainfall, drainage density, slope, and land use.

## 2.6 Flood risk assessment

Flood risk assessment, a vital step in flood management, involves analyzing the function and product of vulnerability and hazard to evaluate the potential impacts of flooding on communities and environments. This information leads to improved policies, decision-making, flood control, and mitigation and adaptation strategies (Peng et al., 2024; Grigg et al., 2023b; Sibandze et al., 2024). However, the risk is a measure of the potential losses that can occur due to the disaster, including loss of life, economic disruption, property damage, and environmental degradation (Helmi, 2020).

Several studies, including those by Gashaw & Legesse (2011) in Ethiopia, Ali et al. (2016) in Egypt, and Bhatt et al. (2014) in India, have effectively demonstrated the usefulness of Geographic Information Systems (GIS) coupled with remote sensing in flood risk management. On the other hand, the article by Muhammad Ihsan Ullah et al. (2024) highlights the importance of integrating advanced hydrological modeling methods and geospatial technologies to produce accurate floodplain maps and assess risks.

Elsebaie et al. 2023, in their study titled “Mapping and Assessment of Flood Risk in the Wadi Al-Lith Basin, Saudi Arabia,” used Geographic Information Systems (GIS) and a multi-criteria decision-making method known as the Analytical Hierarchy Process (AHP) to assess and map flood risk areas. The results revealed that 35.86% of the overall watersheds are potentially vulnerable to high and very high flood risks and 26.85% to moderate flood risk. The study highlighted that the GIS–AHP combination applied to risk assessment is valuable particularly in watersheds that have shortages and scarcity in stream flow gauges and short-interval rainfall measurements. Another study by Boulaghmen et al. (2018), "Management of flood risk in the center of Ghardaia city with a geographic information system (SIG) after the flashflood of 1st October 2008," concentrated on mapping flood-prone areas, using Geographic Information Systems (GIS) and HEC-RAS hydraulic modeling to optimize decision-making. The study emphasized how unchecked urbanization, population pressure, and riverbed occupation make Ghardaia City susceptible to flooding. However, the absence of mitigation and adaptation strategies to deal with the challenges in Ghardaia city is a notable limitation. Furthermore, Waghwala & Agnihotri (2019) pointed out that a transition from a low to a high level of urbanization in Surat City is the main driver for increasing the flood risk.

## 2.7 Analytical hierarchy process (AHP) model

The analytic hierarchy process (AHP) is one of the most popular multi-criteria decision-making (MCDM) methods proposed by Thomas Saaty (Saaty, 1980; Ishizaka & Labib, 2011; Lipovetsky, 2021b). AHP is a structured method for organizing and addressing complicated decision-making issues using mathematics (Tavana et al., 2021). This method provides a precise way for measuring the weights of selection criteria and is a systematic approach to analyze multiple parameters for structuring, organizing, and evaluating complicated judgments (Baalousha et al., 2023). One of the main key benefits of AHP is its logic, simplicity of use, and flexibility, which has been used in almost all the applications related to decision-making, such as business and management, engineering, computer science, social sciences, or mathematics (Madzík & Falát, 2022; Vaidya & Kumar, 2006).

Furthermore, the analytical hierarchy process (AHP) has been extensively utilized to analyze and assess the impacts of flood risk (Mokhtari et al., 2023). According to Siddayao et al. (2014), numerous studies have employed the AHP supported by some additional techniques such as GIS and artificial intelligence (AI) to evaluate food risk assessment. Khaddari et al. (2023) have combined the Analytical Hierarchy Process (AHP) with Fuzzy Logic Modelling (FLM) to assess flood hazards and identify areas prone to flooding. The study weighed several factors into the methodology, such as rainfall amount, land use/land cover (LULC), population, drainage density, distance from the river, elevation, and slope. Moreover, many researchers across the world have integrated the weights obtained from the AHP analysis with geospatial data through a geographic information system (GIS) to create flood risk maps, such as those conducted by Mokhtari et al. (2023) in Algeria, Diriba et al. (2024b) in Ethiopia, Waseem et al. (2023b) in Pakistan, Radwan et al. (2018) in Saudi Arabia, Aydin & Birincioğlu (2022) in Turkey, Aichi et al. (2024) in Morocco, Ahmed et al. (2023) in India, Almouctar et al. (2024b) in Niger, and Aydin & Birincioğlu (2022b) in Turkey. Additionally, the studies indicated that GIS-based AHP is a strong tool for analyzing flood risk, producing flood risk maps, and preparing proper strategies to reduce the vulnerability of hazards (Aydin & Birincioğlu, 2022c; Ahmed et al., 2023).

Although the analytic hierarchy process is a great tool, its methodology that depends on expert judgment in determining factor weights might introduce subjectivity and bias into the decision-making process.

## 2.8 Rainfall-Runoff Models

As one of the most nature destructive calamities, there has been a continuous effort throughout human history to understand, evaluate, and predict flood events and their effects (Teng et al., 2017b; Kumar et al., 2023). To achieve this goal, systematic efforts within the research community have greatly developed the capability of flood inundation modeling since the 1970s. Flood inundation models are a crucial tool to understand the hydrodynamics of flood events and evaluate and analyze risk (Willis et al., 2019). According to Moradkhani & Sorooshian (2008), all rainfall runoff models are simplified representations of real-world systems. A rainfall-runoff model (also referred to as a hydrologic model) is a mathematical representation of the hydrological processes that describe the relationship between rainfall and runoff in a watershed, drainage basin, or catchment area (Trivedi et al., 2018). Planning and developing water structures, predicting floods, assessing water availability, forecasting the effects of climate and land use changes on water, and estimating flow from ungauged catchments are just a few of the many applications for hydrological models (Deb & Kiem, 2020). Rainfall–runoff models are generally classified into conceptual models (parametric models), empirical models (metric models) and physical process-based models (Jehanzaib et al., 2022).

**Table 1:** Comparison of the basic structure for rainfall-runoff models (Sitterson et al., 2018; Jehanzaib et al., 2022).

	<b>Empirical</b>	<b>Conceptual</b>	<b>Physical</b>
<b>Strengths</b>	1. Small number of parameters needed. 2. Limited data requirement. 3. Can be used in Ungauged catchments.	1. Easy to calibrate, simple model structure. 2. Calibrate with limited data. 3. Need less computation.	1. Incorporates spatial and temporal variability, very fine scale. 2. Valid for wide range of situations.
<b>Weaknesses</b>	1. No connection between physical catchment, input data distortion, or Black box.	1. Does not consider spatial variability within catchment. 2. Not recommended for large catchments.	1. Suffer from scale related problems. 2. Large number of parameters and calibration needed; site specific.

---

2. High computation cost and time.			
<b>Models</b>	SCS-CN, ANN, UH	HBV, GR2M, ABCD, TANK, GR4J, SM	TOPMODEL, SWMM, HEC-HMS, WATFLOOD

---

Noteworthy studies, such as those conducted by Bekhira et al. (2019) in Algeria, Jha and Afreen (2020) in the USA, Ongdas et al. (2020) in Kazakhstan, Talukdar et al. (2021) in India, Edamo et al. (2022) in Ethiopia, and Ibrahim et al. (2023) in Somalia, have applied the rainfall-runoff models to estimate inundation. A study by Namara et al, (2021) used the HEC-RAS model to create a flood inundation map of the Awash Bello floodplain in the Upper Awash River basin, and they realized that the whole floodplain is under the influence of flood inundation due to the intensive rainfall event. Another study in Ethiopia applied the ANN and HEC-RAS model for flood inundation mapping, and they successfully improved the accuracy of prediction and flood inundation in lower Baro Akobo River Basin (Tamiru & Dinka, 2021b).

Notably, in Algeria, researchers have been utilizing various models to assess flood risk, such as the HECRAS and HECHMS models. However, very few studies have employed the rainfall-runoff model (RRI). Among the multiple hydrologic models, the RRI model has been chosen to assess flood risk in the Boudouaou watershed and understand flood dynamics.

The Rainfall-Runoff-Inundation model is a two-dimensional model that can simulate flood inundation and rainfall–runoff simultaneously (Sayama et al., 2012). The RRI model considers rainfall–runoff and river flow in the rivers and their interaction, showing overtopping flooding (Sayama et al., 2019). In addition, the RRI model has been developed and used to assess river discharges and flood inundation depths in flood-prone areas (Phyoe & Uchida, 2024b). This model was created by the International Centre for Water Hazard and Risk Management (ICHARM) and developed by Dr. Takahiro Sayama. The 2011 Thailand Flood along the Chao Phraya River had a significant impact through the development of this model. Unlike numerous other flood inundation models, the use of the RRI model is not confined to floodplains. It is applicable to an entire river basin (Sayama et al., 2015).

Several studies have applied the rainfall-runoff-inundation (RRI) model to estimate inundation. Siddiqui et al. (2018) used the RRI model to simulate the 2014 major flood event in the two

eastern, transboundary rivers, the Jhelum and Chenab, in Punjab, Pakistan. The purpose of the research was to identify flood-affected areas using simulated inundation and offer helpful data for emergency response and early warning systems. The model identified the significantly inundated areas along the river, and the simulated and real inundation extents were in good agreement. Moreover, as flash floods are short-lived (less than 24 hours), satellite data was unable to identify the flood-affected area, but the model was able to predict it. Another study in The Bago River has applied the RRI model to assess its applicability for a flat river basin in a data-scarce region and check the accuracy of the modeled inundation maps created for these areas by comparing them with some satellite-based data. The simulated hydrographs demonstrated good results in representing flooding events, and the simulated and measured discharge hydrographs showed good agreement. Additionally, the repeatability of the created inundation maps was satisfactory. Therefore, this study concluded that the RRI model might be suitable for flat river basins like the Bago River basin (Bhagabati & Kawasaki, 2017). Furthermore, Try et al. (2020) evaluated the RRI model by using various gridded precipitation datasets of the whole Mekong River Basin. Thus, APHRODITE, GPCC, and TRMM precipitation datasets were considered suitable for rainfall-runoff and flood inundation modeling. The study also demonstrated the strong performance of the RRI model in the Mekong River Basin. Another study in Cambodia employed the RRI model to identify the flood-prone areas by calculating flood inundation depth and duration. This study aimed to establish mitigation strategies to reduce the risk of flood damage on rice crops in the future in the Stung Sen River Basin (Chung et al., 2019). They confirmed the accuracy of the model by comparing the simulated food inundation areas with food maps generated from satellite imagery. To prevent and mitigate flood damage in the upper Citarum River watershed in Indonesia, Nastiti et al. (2018) used multiple satellite-derived datasets as input data for the RRI model for calibration and verification. The results of this study show that the model effectively identified inundation areas using these datasets compared with the inundation map obtained from JICA and Landsat 7 images.



# CHAPTER THREE: METHODOLOGY

## 3.1 Definition

This study was conducted in the entire Boudouaou watershed located in the northern part of Algeria. In this section, we will provide insights into the elements that characterize the catchment, data collected, software used, and each subsection contribute to a holistic understanding of the watershed and serve as a foundation for detailed analyses of flood risk management.

## 3.2 Study area

### 3.2.1 Geographical Location

The Boudouaou watershed is a sub-basin of the large Algiers coastal basin (02a), located in the northern part of Algeria between the northern latitudes of  $36^{\circ}55'$  and  $36^{\circ}77'$  and the eastern longitudes of  $3^{\circ}37'$  and  $3^{\circ}49'$ . This watershed extends from South to North with an outlet at location coordinates 36.770, 3.420. The main thalweg of Wadi Boudouaou has a total length of 36.34 km.

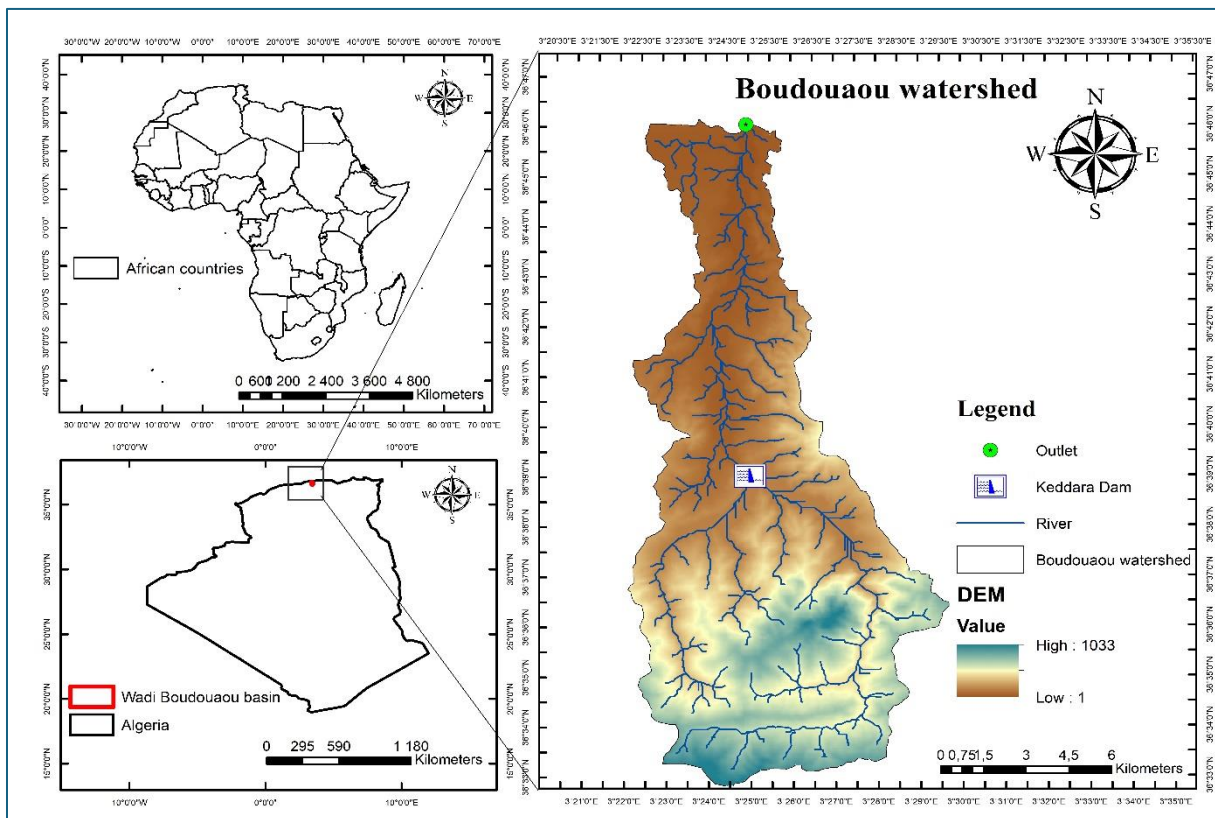


Figure 4: Location of the study area.

### 3.2.2 Topographical and hydrological characteristics

Wadi Boudouaou takes its origin in the heights of the Blidian Atlas, sitting at around 1033 m above sea level, and flows into the northern part of the Boudouaou El Bahri town in the east of Boumerdes before finally discharging into the Mediterranean Sea. The study area's climate is classified as semiarid, where the annual rainfall does not exceed 700 mm. Thus, a local climate can be classified as either a drier, relatively hot lowland climate that experiences significant temperature fluctuations or a rainy, cold mountain climate with relatively low thermal amplitude (Otmame et al., 2024).

### 3.2.3 Geometric characteristics

#### 3.2.3.1 Area and perimeter of the basin

By employing ArcGIS 10.8 software, the tool "Calculate Geometry" and Digital Elevation Model (DEM) data were used to determine the basin's area and perimeter. The controlled area of the Wadi Boudouaou Basin is 149.98 km<sup>2</sup> and a perimeter of 76.89 km.

#### 3.2.3.2 Shape characteristics

##### a) Gravius's compactness index (Kc)

The hydrologists used the Gravius's compactness index (developed by Gravius in 1914) to characterize the watershed shape (Hassani et al., 2021).

$$Kc = 0.28 \frac{P}{\sqrt{A}} \quad (3.1)$$

Where: Kc: Compactness index of Gravius; P: perimeter of the watershed (km); A: watershed surface (km<sup>2</sup>).

$$Kc = 0.28 \frac{76.89}{\sqrt{149.98}} = 1.75 \quad (3.2)$$

Kc = 1.75 (>1) indicates an elongated shape for the Wadi Boudouaou Basin. Additionally, based on the obtained compactness index that exceeds 1.12, the basin can be represented by an equivalent rectangle for a simplified geometric representation.

## b) Equivalent rectangle

This is a purely geometric transformation of the watershed into a rectangle to enable the comparison of watersheds from a hydrological perspective (Boulaghmen et al., 2018). The equivalent rectangle is described by its length "L" and width "W," which are determined by the following formulas:

- **Length (L)**

$$L = Kc \frac{\sqrt{A}}{1.12} \left[ 1 + \sqrt{1 - \left( \frac{1.12}{Kc} \right)^2} \right] \quad (3.3)$$

**L= 33.8 Km**

- **Width (W)**

$$W = Kc \frac{\sqrt{A}}{1.12} \left[ 1 - \sqrt{1 - \left( \frac{1.12}{Kc} \right)^2} \right] \quad (3.4)$$

**W= 4.43 Km**

Where: L: Length of equivalent rectangle (km); W: Width of equivalent rectangle (km); A: Area of basin (km<sup>2</sup>); Kc: Compactness index of Gravelius.

### 3.2.4 Relief characteristics

Relief characteristics are fundamental morphological features of watersheds. Key relief parameters, including elevation and slope, affect hydrological processes such as precipitation distribution, infiltration rates, runoff velocity, and discharge across the catchment landscape (Rai et al., 2017). For instance, steeper slopes facilitate rapid surface runoff, whereas gentle slopes permit more infiltration.

#### 3.2.4.1 Basin elevation

Based on the map (Figure II.6), which represents the distribution of elevations across the Boudouaou watershed, it indicates that the basin encompasses approximately 1033 m of relief (the altitude difference between the highest and lowest points). It clearly highlights mountainous terrain in the upstream, which is characterized by a steep relief and very low to moderate relief in the downstream part of the watershed.

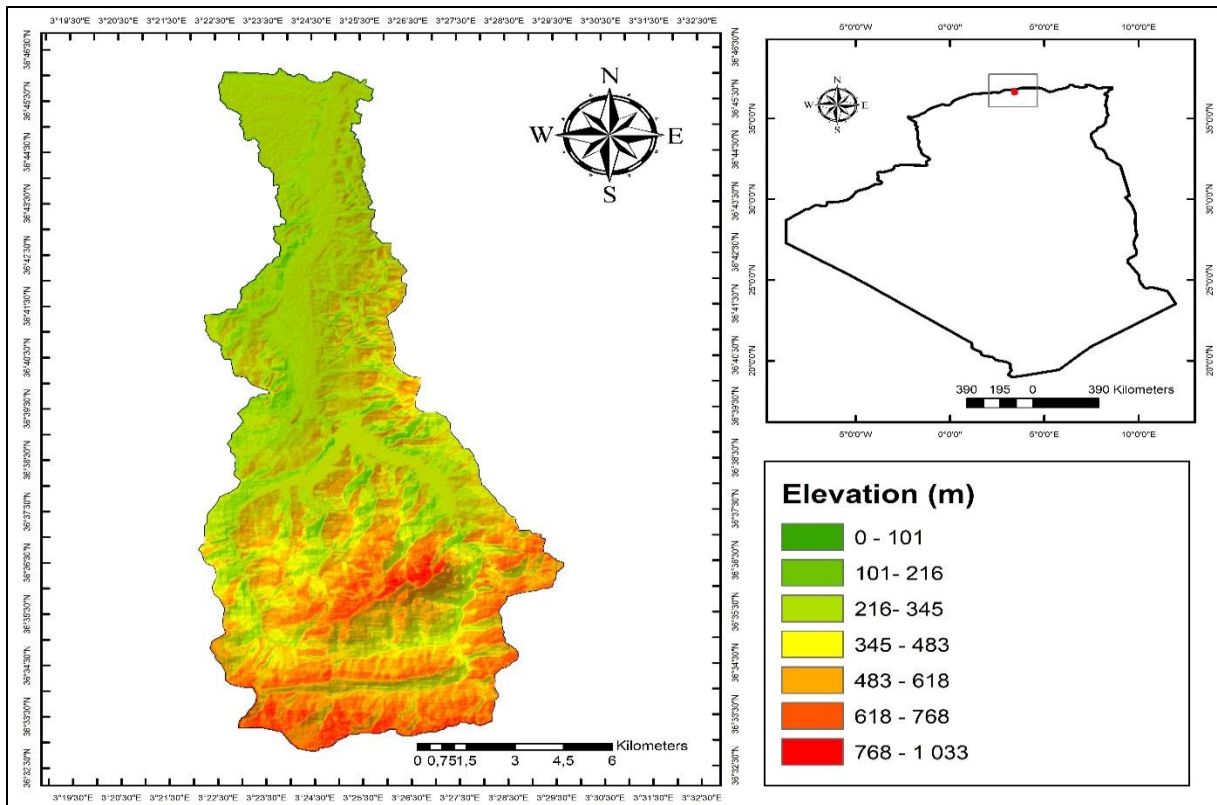


**Figure 5:** Elevation distribution map of the Wadi Khemis Basin.

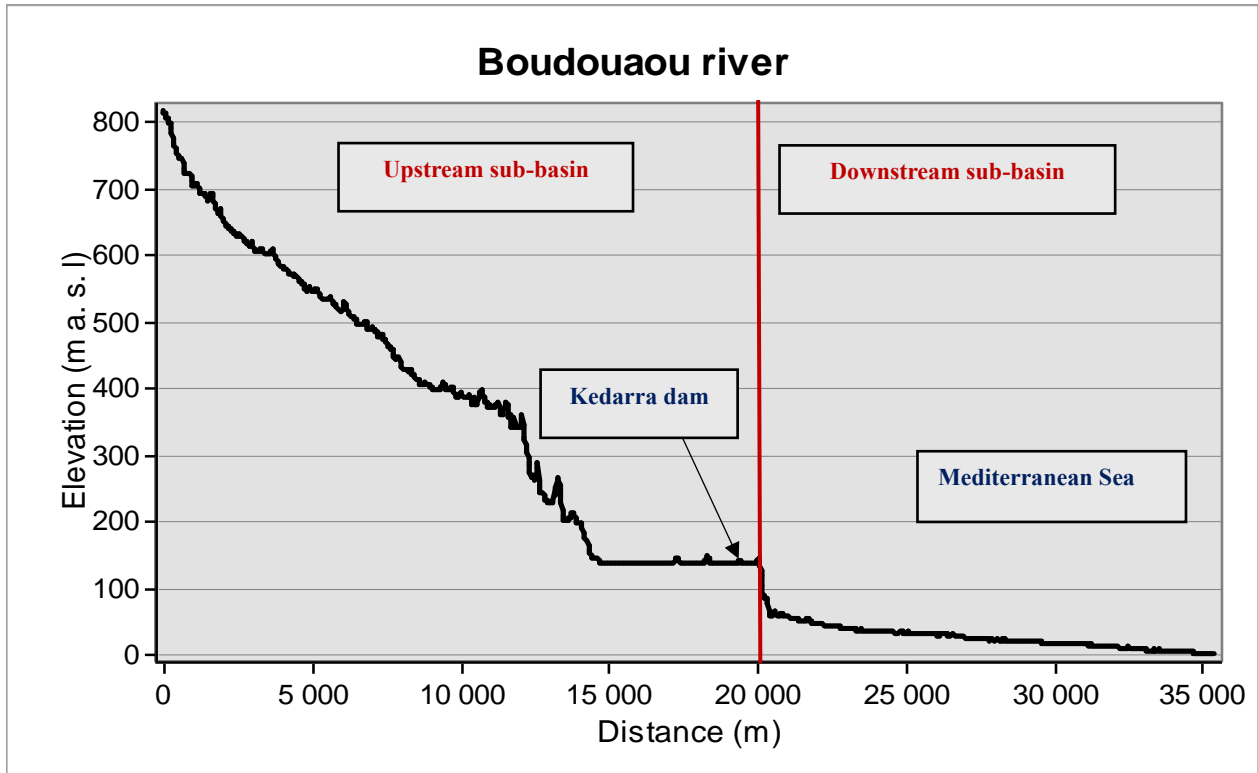


**Figure 6:** Elevation distribution map of the Wadi Khemis Basin.

### 3.2.4.2 Slope

Terrain plays an important role, as it largely controls the ability of land to run off.

#### 3) Global Slope Index (I<sub>g</sub>)

On the hypersonic curve already drawn, points are taken such that the upper or lower surface is equal to 5% of the total surface (Boulaghmen et al., 2018).

$$I_g = \frac{(H_{5\%} - H_{95\%})}{L} \quad (3.5)$$

Where: I<sub>g</sub>: Global slope index (m/km); H<sub>5%</sub>: Elevation exceeded by 5% of basin area (m); H<sub>95%</sub>: Elevation exceeded by 95% of basin area (m); L: Length of equivalent rectangle (km)

**I<sub>g</sub> = 0.0225 m/km (2.25%)**

Based on the ORSTOM classification (Table 3.4), the computed global slope index of I<sub>g</sub> = 0.0225 for the Wadi Boudouaou Basin falls within the range of 0.02 < I<sub>g</sub> < 0.05 indicative of strong enough relief.

**Table 2:** Classification of relief according to (I<sub>g</sub>) given by ORSTOM (Source: Msatef et al., 2018).

Relief	Value of I <sub>g</sub>
Very low relief	I <sub>g</sub> < 0.002
low relief	0.002 < I <sub>g</sub> < 0.005
Rather weak relief	0.005 < I <sub>g</sub> < 0.01
Moderate relief	0.01 < I <sub>g</sub> < 0.02
Strong enough relief	0.02 < I <sub>g</sub> < 0.05
Strong relief	0.05 < I <sub>g</sub> < 0.5
Very strong relief	0.5 < I <sub>g</sub>

#### b) Slope distribution

The analysis of the slope distribution map depicted in Figure 3.7 elucidates a significant spatial variation in the slope gradient across the Boudouaou watershed. The upstream, characterized by a relatively steep slope, increases the speed at which floods propagate and results in a short time concentration. However, as we move from the upstream to the downstream sub-basin, the slope gradient exhibits a marked decrease and becomes gentler, which means a slow time of concentration.

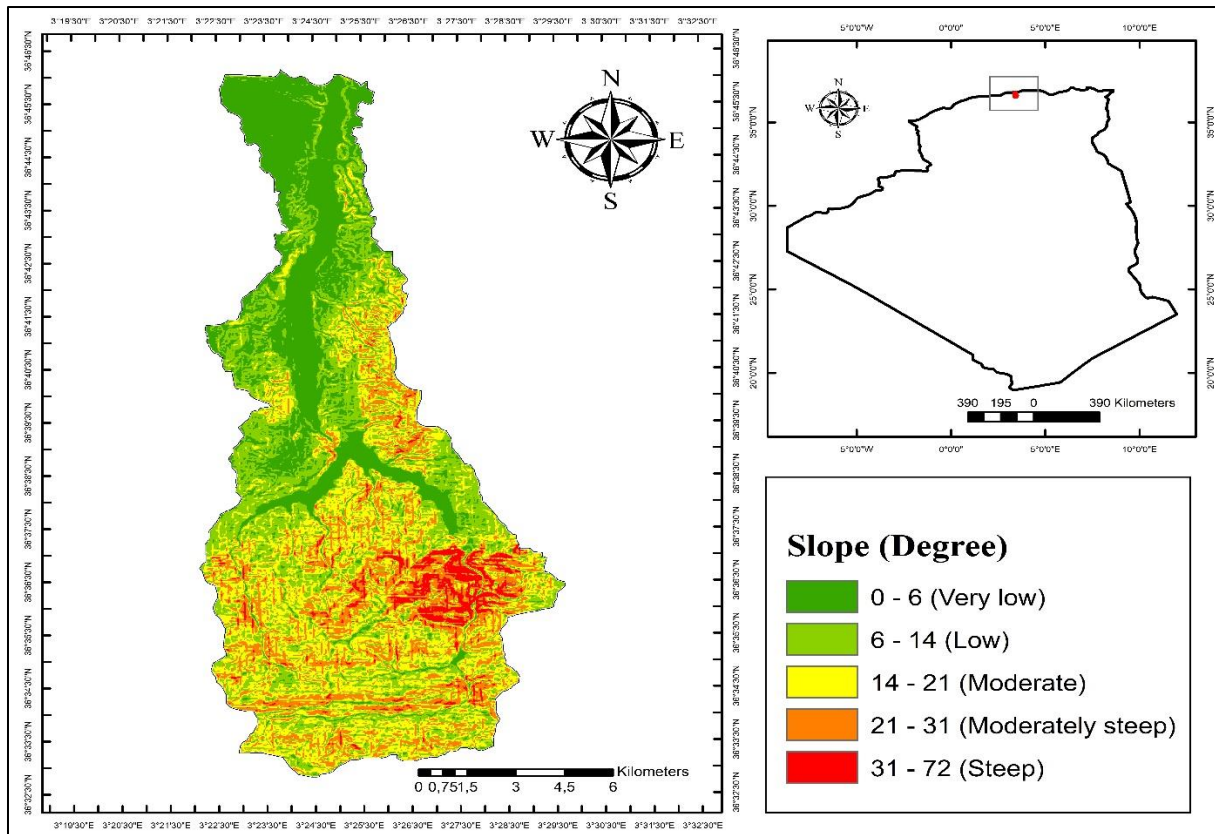


**Figure 7:** Slope distribution map of the Wadi Boudouaou Basin.

**Table 3:** Physical characteristics of Boudouaou Watershed.

Parameters	Symbol	Values	Unit	
Controlled area	A	149.98	km <sup>2</sup>	
Perimeter	P	76.89	km	
Length of the Principal Channel	L	36.34	km	
Gravilius's compactness index	K <sub>c</sub>	1.75	-	
Drainage density	D <sub>d</sub>	1,41	Km/km <sup>2</sup>	
Global Slope Index	I <sub>g</sub>	2.25	%	
Equivalent rectangle	Length	L	33.8	km
	Width	W	4.43	km
Characteristic altitudes	Maximum	-	1033	m
	Minimum	-	0	m

### 3.3 Data collection

Various datasets collected from various sources were needed, as shown in Table 3- 1 below.

**Table 4:** Data Type and source.

<b>Tye of data</b>	<b>Range</b>	<b>Source of the data</b>	<b>Description</b>
<b>Observed rainfall data (Daily)</b>	<ul style="list-style-type: none"> <li>▪ 1971- 2019</li> <li>▪ 1975-2019</li> <li>▪ 1985-2013</li> </ul>	National Agency for Water Resources (ANRH), Algiers.	Precipitation (mm)
<b>River discharge data (Daily)</b>	<ul style="list-style-type: none"> <li>▪ 1973-2009</li> <li>▪ 1983/ 2007</li> </ul>	National Agency for Water Resources (ANRH), Algiers.	Stream flow discharge (m3 /s)
<b>Digital Elevation Model (DEM)</b>		<a href="https://earthexplorer.usgs.gov/">https://earthexplorer.usgs.gov/</a>	
<b>Land use/ Land cover</b>	2023	Esri   Sentinel-2 Land Cover Explorer	Imagery of LULC, reclassified for the year 2023. Resolution: 10m

### 3.3.1 Rainfall data

The acquisition of meteorological data is fundamental for conducting flood hazard analysis within the Wadi Boudouaou Basin. Daily precipitation data used in this study were obtained from the hydrometeorological database maintained by the National Agency for Water Resources (ANRH).

**Table 5:** Rainfall stations in the Boudouaou basin.

	<b>Station code</b>	<b>Latitude</b>	<b>Longitude</b>	<b>Start date</b>	<b>End date</b>	<b>Missing data (%)</b>	<b>Name of the stations</b>
A	020632	557.8	382.25	1/1/1971	31/12/2019	0.0	REGHAIA
B	020646	564.35	372.25	1/1/1975	31/12/2019	2.7	KEDDARA DAM
C	020647	569.15	384.4	1/1/1985	31/12/2014	13.4	BOUMERDES

### 3.3.2 Discharge data

Daily streamflow measurements encompassing the 1973-2009 and the 1983-2007 periods (expressed in cubic meters per second, m<sup>3</sup>/s) for the Ouled-Ali and Pont D-9 gauging stations, respectively. The data were sourced from the National Water Resources Agency (ANRH). The table below describes the hydrological data utilized in this study.

**Table 6:** Discharge stations in the Boudouaou basin.

<b>SN</b>	<b>Sation code</b>	<b>Latitude</b>	<b>Longitude</b>	<b>Start date</b>	<b>End date</b>	<b>Missing data (%)</b>	<b>Name of the station</b>
<b>A</b>	020627	371.55	552.85	1/1/1973	31/12/2009	5.56	OULED-ALI
<b>B</b>	020629	373.02	556.29	1/1/1983	31/12/2007	12.00	PONT D-9

### 3.3.3 Remote Sensing Data

#### 3.3.3.1 Digital Elevation Model (DEM)

A 30 m resolution digital elevation model (DEM) was obtained from the United States Geological Survey (USGS) website (<https://earthexplorer.usgs.gov/>), which is sufficient to capture the terrain features and floodplain details of the study area. The data was then processed in the ArcGIS environment, wherein its projection was WGS\_1984\_UTM\_Zone\_31N. Flow

accumulation and flow direction maps, two input datasets for the rainfall-runoff inundation (RRI) model, were derived to support hydrological modeling.

### 3.3.3.2 Land use/cover

The study obtained a classified land use land cover (LULC) map for Algeria 2023, with a resolution of 10 meters, from the Esri Sentinel-2 Land Cover (<https://livingatlas.arcgis.com/landcover/>). The data includes categories such as urban areas, agricultural land, forests, and water bodies, which are essential for modeling surface runoff. The subsequent step involved extracting the Boudouaou watershed from the dataset and reprojecting it to the WGS\_1984\_UTM\_Zone\_31N coordinate system. The distribution of land cover in the Wadi Boudouaou Basin, as depicted in Figure 3.5, encompassed a diverse landscape of various land cover types. The upstream part of the watershed reveals a dominant presence of tree cover and rangeland, while the downstream sub-basin characterizes a high percentage of built area and cropland.

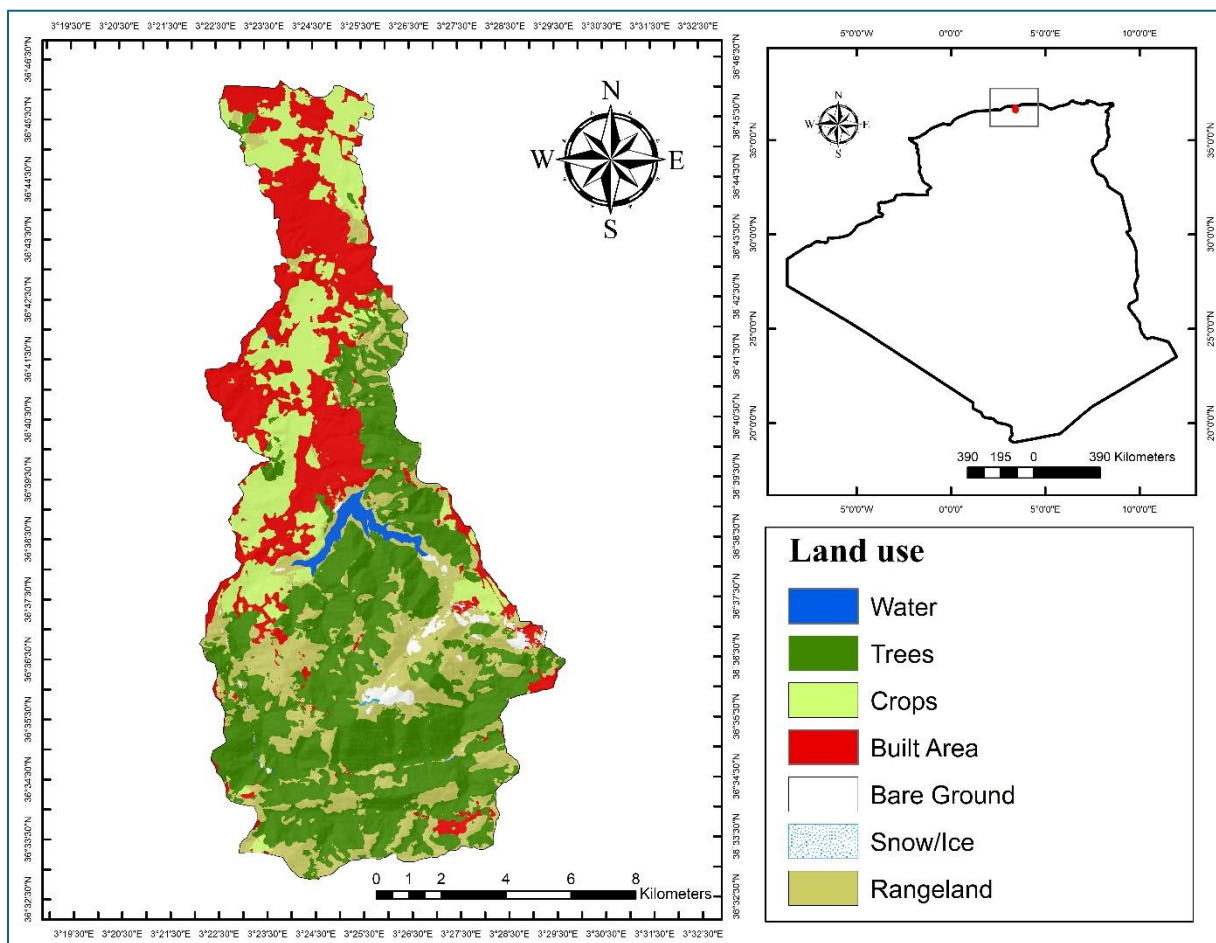


**Figure 8:** Land use/cover distribution within the Wadi Boudouaou Basin in 2023 derived from the 2023 Esri Sentinel-2 Land Cover.

### 3.4 Software required for the processing of data

#### 3.4.1 ArcGIS

ArcGIS Desktop 10.8 was used for the preprocessing and analysis of spatial data, including DEM and land use data into formats readable by the Rainfall Runoff Inundation (RRI) Model.

#### 3.4.2 Rainfall-Runoff Inundation Model

RRI 1\_4\_2\_7 was the primary tool for simulating rainfall-runoff processes and flood inundation. The Command User Interface (CUI) and Graphical User Interface (GUI) are the two interfaces available for this concept. The CUI interface was used in this study.

The RRI model has advanced significantly during the last ten years, leading to a sizable body of academic literature. The RRI model is an advanced two-dimensional hydrological and inundation model that was created by the International Center for Water Hazard and Risk Management (ICCHARM) with assistance from UNESCO (Afra et al., 2025). Fig. 1 shows the schematic diagram of the RRI model.

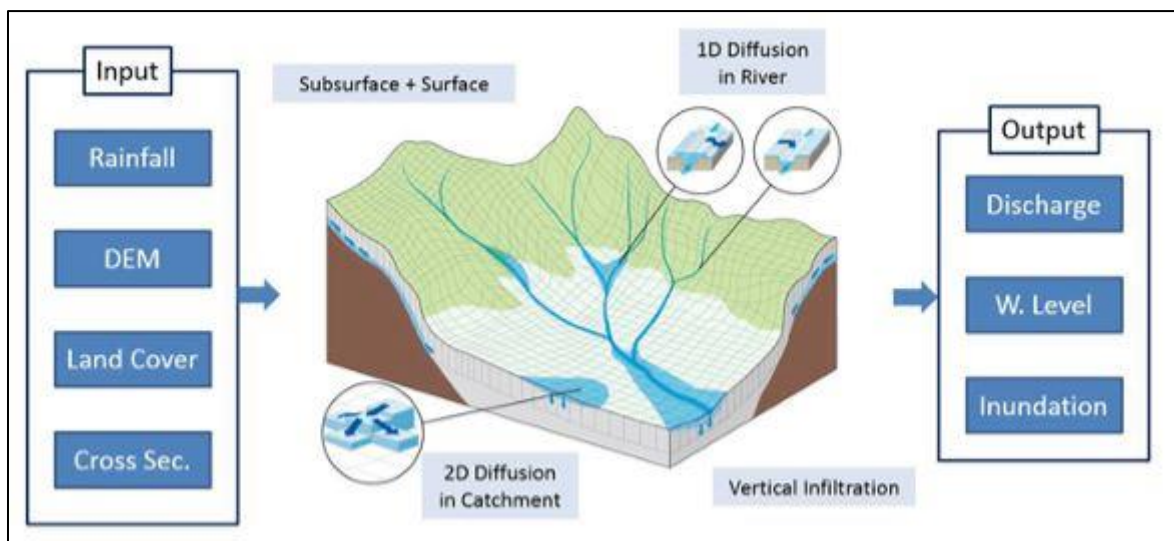


**Figure 9:** Schematic diagram of the rainfall–runoff–inundation (RRI) model.

Three groups of working stages make up the schematic diagram of the operational RRI model shown in Figure 1. Data or information from the target watershed is entered in the first step. Along with the methods or equations used to simulate water flow in the watershed, the second stage is the simulation stage. The extraction of output data, including discharge data, water level, and inundation area, from the simulation results procedure is the final step (Ikhwali et al., 2023).

Assuming that the river channel and slope are located within the same grid cell, the RRI model treats slopes and river channels as separate entities, thereby enhancing accuracy in complex topographical settings (Sayma, 2014). The one-dimensional diffusive wave model is used to mimic channel flow, while the two-dimensional diffusive wave model is used to simulate runoff on the slope (Afra et al., 2025). The model simulation considers lateral subsurface flow, vertical infiltration flow, and surface flow for better representation of real rainfall-runoff-inundation processes (Try et al., 2018). The model uses the mass balance expression below:

$$\frac{\partial h}{\partial t} + \frac{\partial q_x}{\partial x} + \frac{\partial q_y}{\partial y} = r - f \quad (3.6)$$

where  $h$  [L] is the height of water from the local surface;  $q_x$  and  $q_y$  are the unit-width discharges in the  $x$  and  $y$  directions, respectively; and  $f$  represents the infiltration rate.

River grid cells are modeled using a one-dimensional diffusive wave approach. It is assumed that the geometry is rectangular, with width  $W$ , depth  $D$ , and embankment height ( $H_e$ ) is defining its shapes (Nastiti et al., 2018). The following power equations are used to approximate the river's width [ $W$  (m)] and depth [ $D$  (m)]:

$$D = C_D A^{S_D} \quad (3.7)$$

$$W = C_W A^{S_W} \quad (3.8)$$

$C_D$  and  $S_D$  are the geometry parameters for the river depth power equation,  $C_W$  and  $S_W$  are the geometry parameters for the river width power equation, and  $A$  is the watershed area (km<sup>2</sup>).

### 3.4.2.1 RRI Model Input

The RRI model operates on the integration of hydrological and hydraulic processes, relying heavily on the quality and comprehensiveness of its input data to ensure precise simulations. In general, the set of data used in the RRI model can be described by several components that vary and influence the success of the model in the identification of the trends in floods (Sayama et al., 2012).

#### a. Preparation of input rainfall data

Rainfall is the most important input data for the RRI model (Try et al., 2018). For this study, daily rainfall data were obtained for the simulation period and prepared in an Excel sheet in the format below. A rainfall input file needs to be saved in the csv format. Excel or a text editor can prepare the file (saved as CSV).

1	A	B	C	D	E	F	G	H	I	J	K	L	M	N	O	P
2	lat	-7.1945	-7.12661	-7.06353	-7.22057	-7.2496	-6999	-7.23782	-7.24462	-7.19658	-7.19815	-7.25191	-6999	-7.17517	-7.19885	-7.25725
3	lon	111.854	112.1116	111.5464	111.1082	111.8431	-8998	111.5085	111.8725	112.0301	111.8285	111.4878	-8998	112.0616	112.086	111.8287
4	2007/12/24 0:00	0	0	0	0	0	0	0	0	0	0	0	0	0	0	0
5	2007/12/25 0:00	15	5	14	0	2	2	6	0	0	0	0	2	3	9	1
6	2007/12/26 0:00	46	40	52	42	85	61	30	65	68	59	70	48	4	40	61
7	2007/12/27 0:00	0	0	0	0	0	0	0	0	0	0	16	0	0	0	0
8	2007/12/28 0:00	14	5	15	0	5	8	0	3	0	0	11	5	0	11	5
9	2007/12/29 0:00	0	3	3	3	7	0	0	7	8	0	0	0	0	0	8
10	2007/12/30 0:00	8	0	0	0	0	0	0	0	0	0	0	2	0	0	0
11	2007/12/31 0:00	16	2	9	0	8	2	0	4	0	15	0	1	5	0	2
12	2008/1/1 0:00	0	0	0	0	0	0	0	0	0	0	0	0	8.5	0	0
13	2008/1/2 0:00	4	7	8	0	0	0	0	4	3	0	3	0	0	2	0
14	2008/1/3 0:00	6	0	7	0	0	0	3	0	0	0	0	0	6	0	4
15	2008/1/4 0:00	8	0	25	15	20	22	0	25	2	20	0	5	3	10	16
16	2008/1/5 0:00	9	13	0	2	15	0	20	0	0	0	0	7	0	0	0
17	2008/1/6 0:00	0	0	0	0	0	0	0	0	0	0	0	0	34	0	8
18	2008/1/7 0:00	42	0	2	0	0	0	10	0	0	0	0	0	2	0	0
19	2008/1/8 0:00	8	8	37	3	5	22	0	6	12	30	0	40	7.5	0	31

The date and time are listed in the first column of the file (L4-). At the moment, the time and date must be entered as "yyyy/mm/dd h:mm." A rainfall input file needs to be saved in the CSV format. Excel or a text editor can prepare the file (saved as CSV).

**b. Preparation of topographic data**

Digital Elevation Model (DEM), flow direction (DIR) and flow accumulation (ACC) were the topography input for RRI Model. Using ArcGIS, a Digital Elevation Model (DEM) downloaded from the USGS can be processed to derive valuable hydrological information. Initially, a DEM is usually filled to eliminate fictitious sinks or depression-less areas that disrupt flow. Following that, the Flow Direction tool is employed to determine the water flow from each cell to the steepest downslope neighbor. From this step, a flow direction raster is created where every cell is assigned a value representing the direction of flow. Subsequently, the flow accumulation tool employs the flow direction raster to compute the accumulated flow for each cell. Noted that the RRI model does not use flow direction and accumulation for flood routing because the flow direction varies based on local hydraulic gradients. Instead, it uses these factors only to determine the locations of river channels. The DEM, flow accumulation, and flow direction (Figure 3-6) were then extracted using the watershed raster. The files were transformed into the ASCII format that the RRI model could read, with comparable numbers of rows, columns, and cell sizes.

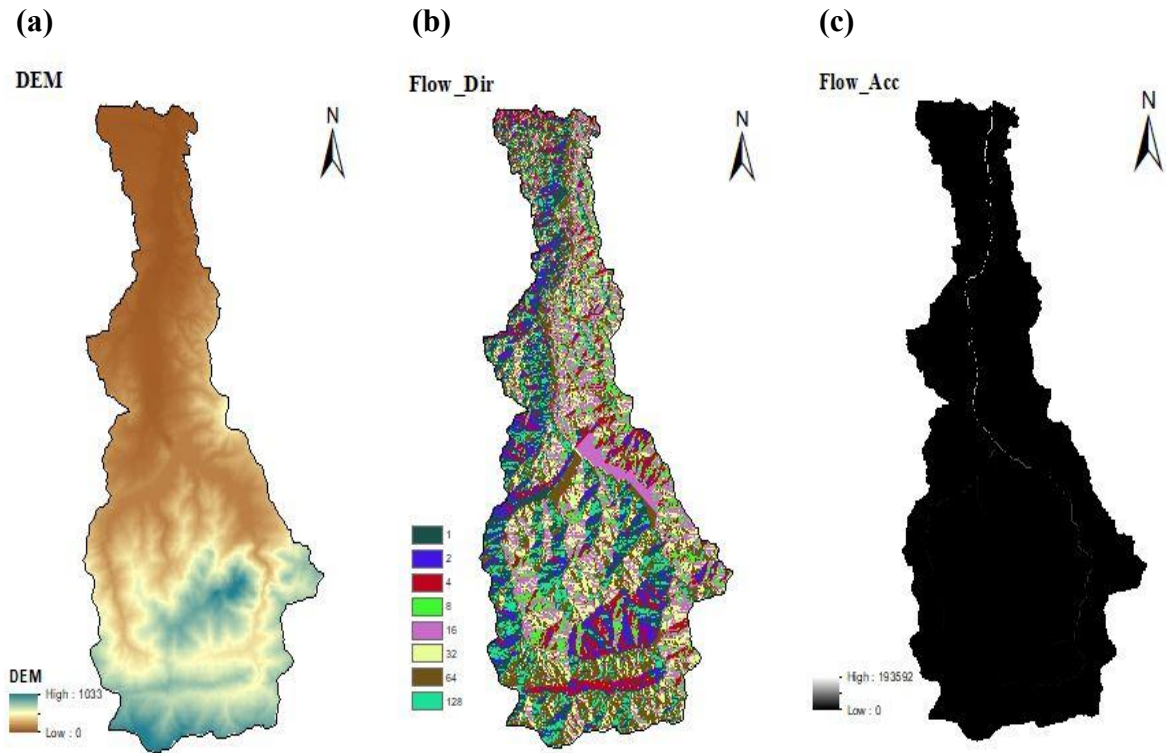


**Figure 10:** Topographical characteristics of the Nan River Basin. (a) Topography; (b) Flow direction; and (c) Flow accumulation.

The river cross-section was confirmed to be the sensitive parameter for the RRI model. As the reliable surveyed data for the river cross-section could not be obtained, the following regression was used (Nastiti et al., 2015):

$$\text{Width (m)} = 5A^{0.35} \quad (3.9)$$

$$\text{Depth (m)} = 0.95A^{0.2} \quad (3.10)$$

where  $A$  ( $\text{km}^2$ ) implies the area upstream that contributed to flow.

### c. Preparation of the land use/land cover map

land use land cover (LULC) map for Algeria 2023 from the Esri Sentinel-2 Land Cover was imported into the Geographic Information System (GIS) environment as a shapefile. Considering the dataset's extensive coverage, I first extracted a rectangular area encompassing my watershed to reduce processing time and data volume. This extraction of land cover data also needed to ensure that it had the same resolution, cell size, and other spatial properties as the Digital Elevation Model, flow accumulation, and flow direction rasters. using my defined watershed boundary polygon and a geoprocessing tool to precisely extract the land use data specific to my watershed. The resulting raster file was then converted to an ASCII format. The

original land use/land cover map consisted of seven land classes, namely, built area, crops, trees, bare area, rangeland, water and snow/ice.

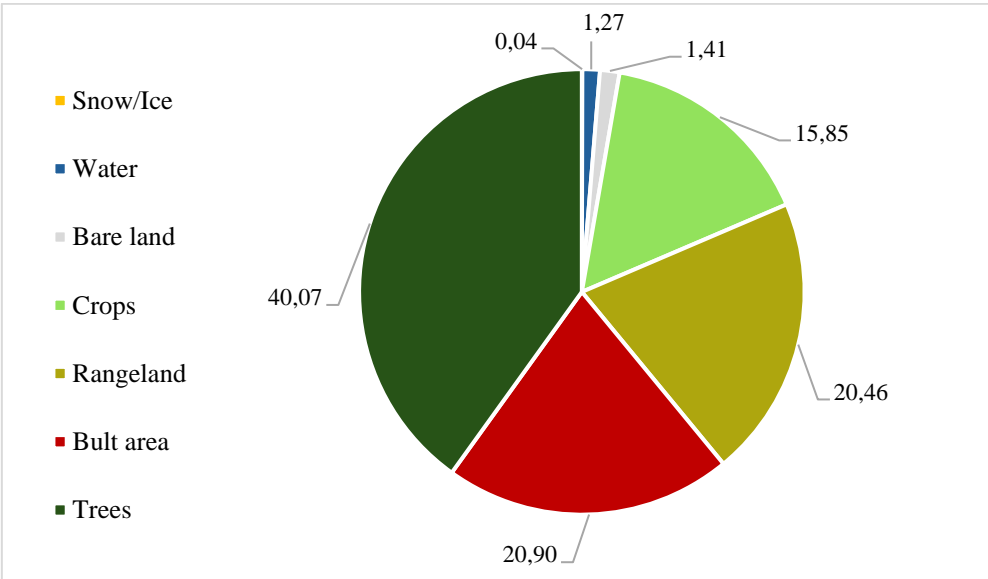
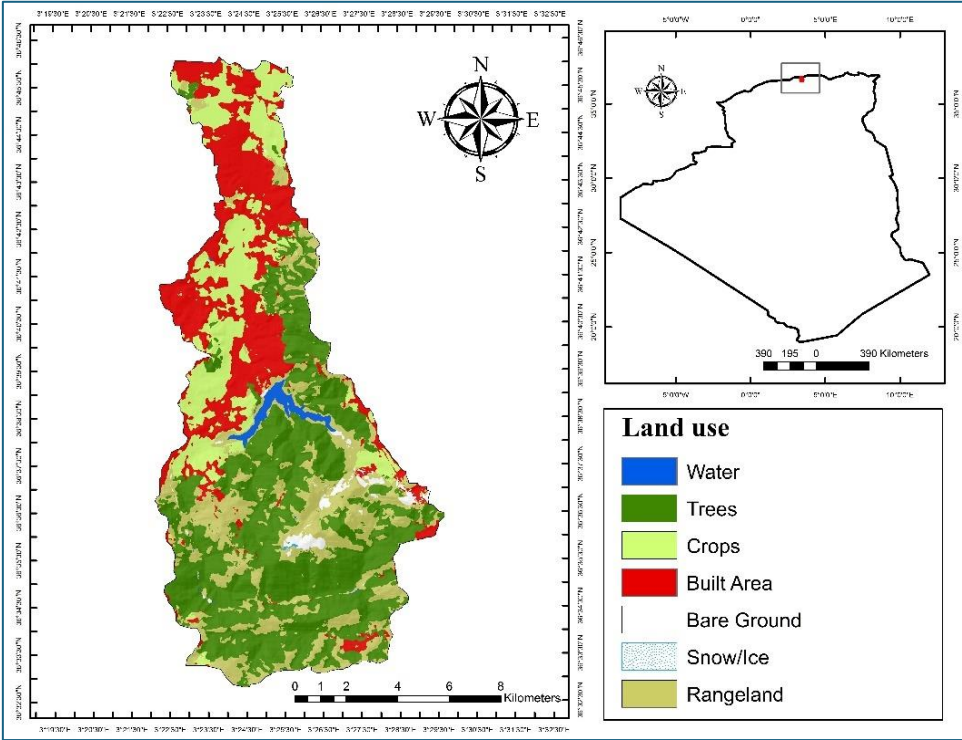


**Figure 11:** Percentage of land use/land cover types within Wadi Boudouaou watershed.

**3.4.2.2 Model simulation**

The Rainfall–Runoff–Inundation (RRI) model is widely used for flood simulation, integrating rainfall-runoff processes and inundation dynamics within a single framework. Flood risk assessment relies on a variety of modeling approaches, each with distinct strengths and

limitations. In order to simulate stormwater runoff and the flood inundation process during intense storm events, a study conducted by Liu et al. (2015) develops an efficient and flexible cellular automaton (CA) model. This model included transition rules based on water supply and demand and considered a variety of metropolitan settings. According to Gholami and Khaleghi (2022), the ANNs empirical model shows effectiveness in predicting rainfall-runoff under conditions of limited data availability. However, their reliance on historical data and limited representation of physical processes can be a constraint. The requirements for large computational power in physically based distributed models lead to stronger simulation capabilities of complete hydrological procedures. While models like the WEB-RRI (Rasmy et al., 2019) integrate water and energy budgets for improved process representation, they can be computationally demanding.

This study utilizes the two-dimensional Rainfall-Runoff-Inundation (RRI) model due to its balance between the ability to simulate flood inundation and rainfall-runoff simultaneously and its balance between computational efficiency that provides essential spatial data needed for hazard assessment (Sayama et al., 2012). Within its grid-based operation, the model calculates both slope flow and channel flow, thus producing more realistic flood propagation results. The RRI model requires key hydrological data, including rainfall, digital elevation models (DEMs), and land use. The cross-sectional geometry, river channel calibration, and validation are typically performed using observed discharge data to ensure accuracy. The model's simulation approach included the following steps: data processing, model simulation, model calibration, area inundation and streamflow validation, and flood hazard mapping.

### **3.4.2.3 Model calibration and validation**

Calibration is the process of fine-tuning a model by improving the hydrometeorological data input and optimizing the model parameters through changes to the boundary conditions and model structures (San et al., 2020). Optimization of the parameter value is performed manually and checked qualitatively. The calibration's goal is to adjust some model parameters in order to reduce the discrepancy between the simulated and observed discharge. This study involves adjusting model parameters, such as Manning's roughness coefficient (representing flow resistance), infiltration parameters, soil properties (influencing water storage and flow), and channel geometry (defining river shape and dimensions), to achieve the best match between simulated results and observed data. Model validation is the process of testing the model's ability to simulate the observed data within acceptable accuracy. The calibrated model

parameter values are kept constant during this procedure. Calibration and validation of the RRI model was done by adjusting the Manning's roughness and depth of the soil and infiltration parameters (estimated from Green-Ampt infiltration parameters).

In this study, the accuracy between the simulated and observed runoff during both the calibration and validation stages was evaluated using the Nash–Sutcliffe coefficient efficiency (ENS) and coefficient of determination ( $R^2$ ):

$$\text{NSE} = 1 - \frac{\sum_{i=1}^n (Q_{\text{obs}} - Q_{\text{sim}})^2}{\sum_{i=1}^n (Q_{\text{obs}} - \bar{Q}_{\text{sim}})^2} \quad (3.11)$$

Where:

$Q_{\text{obs},i}$  = observed runoff at time step  $i$

$Q_{\text{sim},i}$  = simulated runoff at time step  $i$

$\bar{Q}_{\text{obs}}$  = mean of observed runoff

$n$  = total number of observations

$$R^2 = \frac{\sum_{i=1}^n (Q_{\text{obs}} - \bar{Q}_{\text{obs}})(Q_{\text{sim}} - \bar{Q}_{\text{sim}})^2}{\sum_{i=1}^n (Q_{\text{obs}} - \bar{Q}_{\text{obs}})^2 \sum_{i=1}^n (Q_{\text{sim}} - \bar{Q}_{\text{sim}})^2} \quad (3.12)$$

Where:

$\bar{Q}_{\text{sim}}$  = mean of simulated runoff

### 3.5 Flood Hazard mapping

Flood hazard mapping involves multiple steps, from data collection and preparation, through model calibration and validation, to the simulation of rainfall-runoff processes and flood inundation. The final output is a flood hazard map classifying areas into low, medium, and high hazard zones based on flood depth.

### 3.6 Flood Vulnerability mapping

Several physical vulnerability characteristics were used in this study to apply the flood-causing elements that were taken into consideration when creating the vulnerability map for the current scenario. The social and economic parameters were excluded due to the lack of data. The variables need to be converted into standard units and incorporated into a spatial database prior to gathering the criterion maps in a GIS environment. This is due to the fact that they are depicted using disparate dimensional scales. A linear fuzzy set membership function was used

to standardize the vulnerability model's criteria, where; vulnerability varies linearly from 0 (no vulnerability) to 1 (total vulnerability) (Mourato et al., 2023). The resulting vulnerability maps were ranked using five equally divided categories: very low, low, moderate, high, and very high. The classification is based on the literature. The methodology can be broken down into the following four sections (Tempa., 2022):

1. Identify the main goal (weighting to FV indicators according to the level of hazard and impact).
2. Formulate criteria (physical/economic, social and environmental).
3. Priorities sub-criteria by AHP pair-wise comparison (population, land use, rainfall)
4. aggregate weighting of the criteria according to the very high, high, medium, low, and very low vulnerability scales.

**3.7 Analytical Hierarchical Process (AHP) method**

Selecting the decision criteria is the first step in the AHP. The alternatives are then evaluated based on the selected criteria (Tavana et al., 2021). In order to determine the weights of the parameters taken into consideration, this study used three important steps: creating a pairwise comparison matrix, normalizing the pairwise comparison matrix, and calculating consistency.

**3.7.1 Pairwise comparison matrix**

The evaluation spectrum spans from one to nine, indicating that a score of one signifies the two components are identical or have the same level of significance. Conversely, a score of nine suggests that one component is vastly more significant than its counterpart in a two-element matrix (e.g., how much more important one criterion is than another) (Seejata et al., 2018).

**Table 7:** Scores for the importance of variable.

<b>Importance Scale</b>	<b>Definition of Importance Scale</b>
<b>1</b>	Equally Important Preferred
<b>2</b>	Equally to Moderately Important Preferred
<b>3</b>	Moderately Important Preferred
<b>4</b>	Moderately to Strongly Important Preferred
<b>5</b>	Strongly Important Preferred
<b>6</b>	Strongly to Very Strongly Important Preferred
<b>7</b>	Very Strongly Important Preferred

8	Very Strongly to Extremely Important Preferred
9	Extremely Important Preferred

The matrix elements can be represented as follows:

$$\mathbf{A} = [\mathbf{a}_{ij}] = \begin{bmatrix} \mathbf{a}_{11} & \mathbf{a}_{12} & \cdot & \mathbf{a}_{1n} \\ \mathbf{a}_{21} & \mathbf{a}_{22} & \cdot & \mathbf{a}_{2n} \\ \cdot & \cdot & \cdot & \cdot \\ \mathbf{a}_{n1} & \mathbf{a}_{n2} & \cdot & \mathbf{a}_{nn} \end{bmatrix} \quad (3.13)$$

Where; A represent the decision matrix,  $a_{ij}$  are comparisons between elements  $i$  and  $j$  for all  $i, j \in \{1, 2, \dots, n\}$ .

In Analytic Hierarchy Process-based flood risk assessment, the pairwise comparison matrix helps determine the relative importance of different factors contributing to flooding and assigns numerical values to represent their relative importance. A matrix-based analysis determines the weight values for individual factors that influence flood risk assessment outcomes. The parametrization of this study was done based on previous literature from similar studies carried out.

With the use of AHP, we are able to obtain a relative significance of the relevant factors after pairwise-comparison matrix have been constructed. The weights of each parameter are defined after they are ranked according to their relative importance.

### 3.7.2. Normalized pairwise comparison matrix.

The elements in each column are divided by the sum of the items in that same column to standardize the matrix for weighing each criterion. The new matrix's rows average establishes the necessary relative weights for each criterion (Prieto-Amparán et al., 2021). After a given number of pairwise comparisons are made, some discrepancies could appear. The consistency ratio (CR), a metric used to assess the consistency of the weights, is part of the AHP. The consistency index (CI) must be determined first in order to compute the CR (Equation (3.13)):

$$\text{Consistency Index (CI)} = \frac{\lambda_{max} - n}{n - 1} \quad (3.14)$$

Where:  $\lambda_{max}$  represents the eigenvalue of the pairwise comparison matrix,  $n$  denotes the number of the criteria.

### 3.7.3. Consistency

The consistency ratio (CR) defines the probability that the matrix scores are randomly generated (Mourato et al., 2023). In the next step, in order to validate the AHP results, the CR is calculated to completely measure the consistency in the pairwise comparison using the following formula (Taherdoost, 2017b):

$$CR = \frac{CI}{RI} \quad (3.15)$$

Where CR= CI=consistency index, consistency ratio, and RI= random index varies according to the number of factors used in the pairwise matrix.

The value of Random consistency index (RI) is associated to the dimension of the matrix and will be extracted from Table 3.

**Table 8:** The value of Random Consistency Index.

Dimensions	RI
1	0
2	0
3	0.5799
4	0.8921
5	1.1159
6	1.2358
7	1.3322
8	1.3952
9	1.4537
10	1.4882

The appropriate CR value must be 0.10 or less ( $CR < 0.10$ ) in order to avoid inconsistency and to get meaningful results. The pairwise comparison matrices must be revised if they display a consistency value greater than 0.10 (Tavana et al., 2021; Prieto-Amparán et al., 2021).

### 3.8 Flood Risk Map

To develop the flood risk map for the Boudouaou basin, a multiplicative approach will be applied based on the Kron Equation, where flood risk is calculated as the product of flood vulnerability and flood hazard:

$$\mathbf{Flood\ Risk = Flood\ Hazard \times Flood\ Vulnerability} \quad (3.16)$$

The flood hazard ASCII files generated for the 5-year, 10-year, 25-year, and 100-year return periods were brought into the GIS environment through an ASCII to raster conversion tool. An ASCII to raster conversion program was used to import the flood hazard ASCII files created for the 5-year, 10-year, 25-year, and 100-year return periods into the GIS environment. To match the resolution of the flood vulnerability map, these maps were then resampled. Second, the hazard vector layer was categorized into several categories with different inundation depth ranges (Abdrabo et al., 2020). The final flood risk map will be obtained by multiplying the flood hazard and vulnerability layers, producing a spatial representation of flood risk categorized into different levels (very low to very high). The findings will illustrate how flood risk varies under various rainfall conditions, supporting the development of effective flood mitigation strategies.

### **3.9 Proposed mitigation strategies**

The flood risk assessment results will lead to identifying proposed strategies for minimizing flood impacts. These include structural measures such as flood protection infrastructure, improved drainage systems, and modifications of river channels, and non-structural measures such as land-use planning, early-warning systems, and community awareness programs.

---

**RESULTS AND DISCUSSIONS**

## CHAPTER FOUR: RESULTS AND DISCUSSIONS

### Part 01: Flood vulnerability assessment using AHP method

#### 4.1.1 Introduction

Flood vulnerability assessment is a critical component of flood risk management, enabling the identification of areas most susceptible to flooding. This study applied the integrated AHP–GIS analysis, which consists of four phases. Initially, seven flood hazard parameters were identified and subsequently processed using GIS (elevation, slope, rainfall, TWI, distance from river, and drainage density), followed by the construction of a pairwise comparison matrix to determine the relative importance of each factor. Previous studies on floods play an important role in forming these factors. extracting insights from existing literature and similar studies. Second, AHP was used to weigh the parameters. Third, a consistency check was done by checking the consistency ratio (CR) to ensure the logical consistency of the weight assignments. Finally, the flash flood hazard map of the Boudouaou watershed was developed.

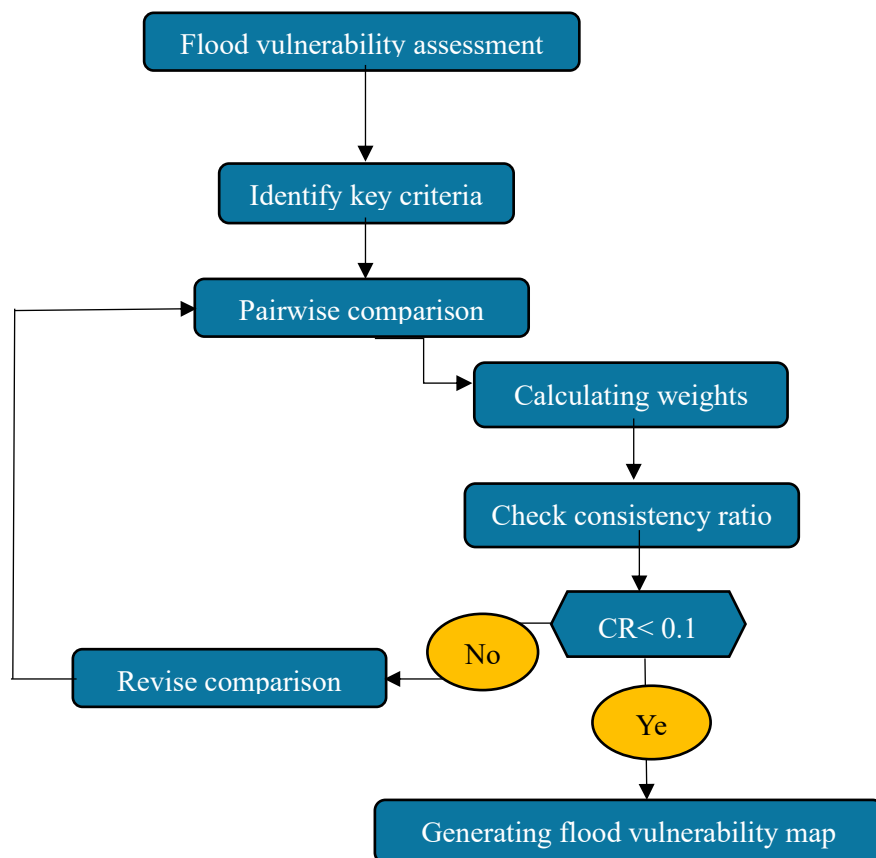


**Figure 12:** Flowchart of Flood Vulnerability Assessment Using Analytical Hierarchy Process (AHP).

## **4.1.2 Flood vulnerability assessment**

Vulnerability is controlled and influenced by various physical and natural factors. These factors have been identified as the criteria for this analysis. Vulnerability is shaped and regulated by various physical and natural factors. In this research, five criteria related to physical vulnerability (Elevation, slope, land use, rainfall, drainage density, distance from the river, and Topographic Wetness Index) were selected for vulnerability assessment.

### **4.1.2.1 Defined the criteria:**

#### **1. Land use:**

Landcover has an important impact on the ability of the soil to act as a water store. It has a direct or indirect effect on the rates of infiltration, evapotranspiration, and the generation of surface runoff. The presence of dense vegetation cover significantly impedes the movement of water and reduces the amount of runoff. Conversely, surfaces that are impermeable, such as concrete, absorb almost no water at all. Roads, houses, and slum areas are examples of land use that reduces the soil's ability to penetrate and increases water runoff. It is crucial to consider the transformations of the land over time, as well as the influences of natural forces and human activities. These practices are recognized as contributing factors to the occurrence of catastrophic natural hazards. This indicates that land use and land cover are vital elements in assessing the likelihood of flooding (Ouma & Tateishi, 2014; Sharir et al., 2022).

#### **2. Elevation**

In the domain of flood mapping, the experts believe that the elevation of a region is the primary factor that controls the flood hazard (Sharir et al., 2022). Elevation plays a crucial role in determining flood vulnerability, with lower-lying areas generally being more vulnerable to floods, particularly in coastal locations. Higher elevation regions, on the other hand, are often less vulnerable to flooding; however, they may encounter different risks, such as landslides, particularly if the landscape is steep and unstable (Koroma et al., 2024). In this study, the map classifies the terrain into five elevation categories: very low, low, moderate, high, and very high. It clearly highlights mountainous terrain in the upstream, which is characterized by steep relief and very low to moderate relief in the downstream part of the watershed. In this study, a higher weighted value was assigned to lower elevation compared to higher elevation. The map classifies the terrain into five elevation categories: very low, low, moderate, high, and very high.

### **3. Slope:**

The accumulation of water at any location is intricately connected to the surface slope, as the slope has a direct impact on the surface water runoff (Rebouh et al., 2024). Floods are typically more likely to occur in flat areas connected to lower slopes. Naturally, lower slopes are categorized as having the greatest level of risk, making them more vulnerable to flood-related threats (Seejata et al., 2018; Kazakis et al., 2015; Vignesh et al., 2020). In this research, the digital elevation model (DEM) and slope generation tools available in ArcGIS software were utilized to produce the slope map. Slope classes with lower values were given a higher rank due to the nearly flat nature of the terrain, while the class with the highest value was assigned a lower rank because of its comparatively high runoff. The slope map was grouped into five classes.

### **4. Drainage Density:**

According to Hammami et al. (2019), drainage density, representing the total length of rivers within a specified area ( $\text{Km}/\text{km}^2$ ), serves as a crucial component of flood control methods. Areas with a high drainage density are more susceptible to flooding than those with a lower drainage density (Sharir et al., 2022). In this study, the drainage density map was generated from the DEM and processed using ArcGIS 10.8 with the Spatial Analyst Tool. The drainage density layer was further reclassified in five levels of susceptibility to flooding. The classifications for these levels included very low, low, moderate, high, and very high, indicating that an increase in drainage density is associated with a greater vulnerability to flooding.

### **5. Distance from the River**

The distance to the main river system is generally associated with the elements that cause river flooding (Rebouh et al., 2024). River overflows are crucial for the initiation of a flood event. Typically, the flooding originates from riverbeds and expands into the surrounding areas (Kazakis et al., 2015). Several studies have observed that locations nearer to drainage systems are more vulnerable to flooding. However, Areas further from the drainage system are typically less prone to flooding. Kazakis et al. (2015) demonstrated that areas located within 200 meters of the river network are extremely vulnerable to flooding, while the impact of this parameter diminishes at distances greater than 2000 meters. Another study by Das (2019a), highlight that areas within 500 meters of the drainage line are most vulnerable to flooding. This analysis categorized the area into five vulnerability classes based on the proximity to rivers: very high, high, moderate, low, and very low.

## **6. Rainfall:**

According to Hammami et al. (2019), rainfall is one of the key climate factors directly influencing flood susceptibility. The risk of flooding increases with the amount of rainfall in a particular area (Marengo et al., 2021). Areas with higher rainfall are more vulnerable to flooding, while those with lower rainfall are less susceptible. The relationship between rainfall and floods is complex and depends on several parameters, including rainfall intensity, duration, and spatial distribution, as well as catchment area characteristics. Heavy rainfall typically increases the amount of water in rivers and streams, which can create flooding if it exceeds the channel's capacity (Breinl et al., 2021).

A critical step in ensuring the accuracy of the flood susceptibility study is the creation of a precipitation map for the study area.

## **7. Topographic Wetness Index (TWI)**

The Topographic Wetness Index (TWI) helps identify locations prone to water accumulation based on their topographic characteristics (Koroma et al., 2024). The Topographic Wetness Index (TWI), derived from topographical data, is one of the significant factors for assessing the impact of terrain features on flooding (Rebouh et al., 2024). The area with a higher topographic wetness index value indicates the high potentiality of a flood event (Hasanuzzaman et al., 2022). As the TWI value increases, so does the likelihood of flood risk. For this study, we created a map of the topographic wetness index using the Spatial Analyst Tool in ArcGIS 10.8, which is divided into five categories: very low, low, moderate, high, and very high. The TWI has been categorized into five classes.

### **4.1.2.2 AHP weighting factors**

#### **A. Construction of the Pairwise Comparison Matrix**

Following the preparation of all thematic layers corresponding to the selected parameters of the factors, the AHP model was used to calculate various weights (shown in Figure 1) that would appropriately represent the impact of each factor on the phenomenon being studied. The study used a  $7 \times 7$  pairwise matrix in AHP to compare the relative significance and find each parameter's weight based on the literature and expert opinions in the field. The important scale varies from 1 to 9, representing less important to much more important criteria, respectively (Khoeun et al., 2022).

**Table 9:** Pairwise comparison matrix.

	<b>Slope</b>	<b>Elevation</b>	<b>rain</b>	<b>LULC</b>	<b>RIV_DIS</b>	<b>RIV_DEN</b>	<b>TWI</b>
<b>Slope</b>	1	1/2	1/4	1/2	1/3	1/2	1/3
<b>Elevation</b>	2	1	1/3	1/2	1/2	2	1/2
<b>rain</b>	4	3	1	2	2	3	3
<b>LULC</b>	2	2	1/2	1	1/2	2	1
<b>RIV_DIS</b>	3	2	1/2	2	1	2	2
<b>RIV_DEN</b>	2	1/2	1/3	1/2	1/2	1	1/2
<b>TWI</b>	3	2	1/3	1	1/2	2	1

#### **B. 4.2.2.2. Calculation of Criteria Weights**

The weights assigned to these criteria are defined after ranking them according to their relative importance (Khoeun et al., 2022). Each factor's weight ( $w_i$ ) was estimated by using Saaty's Method, which involves normalizing pairwise comparison matrix A, and transformed into matrix  $B = [b_{ij}]$ , and computing the arithmetic averages from the row of the normalized comparison matrix B using the following formula:

$$w_i = \frac{\sum_{j=1}^n b_{ij}}{n} \quad (4.1)$$

Where, n is number of elements in the row, and  $b_{ij}$  is the element of matrix B after normalizing pairwise comparison matrix A, defined by equation [14].

$$b_{ij} = \frac{a_{ij}}{\sum_{i=1}^n a_{ij}} \quad (4.2)$$

**Table 10:** Normalized pair-wise comparison and weight values of flood attribute

	Slope	Elevation	rain	LULC	RIV_DIS	RIV_DEN	TWI	Weights
Slope	0,06	0,05	0,08	0,07	0,06	0,04	0,04	0,0558
Elevation	0,12	0,09	0,10	0,07	0,09	0,16	0,06	0,0988
Rain	0,24	0,27	0,31	0,27	0,38	0,24	0,36	0,2939
LULC	0,12	0,18	0,15	0,13	0,09	0,16	0,12	0,1372
RIV_DIS	0,18	0,18	0,15	0,27	0,19	0,16	0,24	0,1952
RIV_DEN	0,12	0,05	0,10	0,07	0,09	0,08	0,06	0,0809
TWI	0,18	0,18	0,10	0,13	0,09	0,16	0,12	0,1383

**C. 4.2.2.3 The consistency ratio**

To ensure the differences between the pairwise comparisons and the reliability weights that were calculated, then the consistency ratio was computed to check the consistency.

**Table 11:** The consistency ratio.

Consistency Index (CI)	RI 7X7	Consistency Ratio (CR)
0,036960933	1,34	0,02758279

**D. 4.2.2.4 Flood Vulnerability index (FVI)**

Thematic representations of all the parameters were created and reclassified after assigning rank to each class using AHP (Table 6). The reclassified thematic layers along with the weighted value of each parameter were used to prepare Flood vulnerability Index (Vignesh et al., 2020). The FVI map was generated in ArcGIS 10.8 software. The formula of FVI is expressed below:

$$FVI = \sum_{i=1}^n W_i \times R_i \quad (4.3)$$

Where  $W_i$  is the weights for individual flood conditioning factors, and  $R_i$  represents the rating of the classified value of each factor.

Finally, the obtained flood vulnerability map was reclassified into five groups: very high, high, moderate, low, and very low.

#### **4.1.3 Results & discussion:**

The flood vulnerability assessment for the Boudouaou watershed relied on seven key criteria: rainfall, distance from rivers, slope, elevation, land use/land cover (LULC), topographic wetness index (TWI), and drainage density to characterize and evaluate areas at risk of flooding. By evaluating these diverse layers, the study gained additional knowledge about the regions that are at risk of experiencing floods in the watershed. Rainfall emerges as a critical factor, especially in the central and southern regions, with areas receiving high to very high rainfall being particularly vulnerable to flooding events. The slope in the watershed ranged from 0 to 72 degrees, with the highest vulnerability associated with slopes between 0 and 14 degrees classified as very high and high risk, represent a gentle slope, which prone to prolonged water stagnation and increased inundation duration. This vulnerability is further accentuated by elevation, which varied from 0 to 1033 meters. More than 50% of the watershed is below 313 meters that serve as accumulation zones for floodwaters, falling within the "high" to "very high" vulnerability categories, further amplifying flood susceptibility in these low-lying regions. The land use/land cover map shows that a majority of the total upstream area is covered by trees and rangeland, which allow greater water absorption and flood mitigation. Additionally, urbanized and impermeable surfaces reduce natural infiltration and accelerate surface runoff in the downstream area with a total area of 20.90% due to human-induced landscape alterations. The aforementioned vulnerability is further compounded by river channel proximity, which was a determining factor of vulnerability, as areas nearest to rivers registered extremely high rates of vulnerability because of direct exposure to flood occurrences. Topographic wetness index (TWI) also reinforced these results by highlighting individual sites that are prone to saturation with water, correlating closely with areas in proximity to streams and rivers. Finally, drainage density acted as an integrative factor of significant value in signaling the impact of dense stream networks because these areas have multiple streams that flow to each other and eventually join the Boudouaou Wadi.

**Table 12:** Flood Vulnerability Factors and Rating Scale.

N°	Factors	Class	Descriptive level	Rating
1	Slope	0 – 6	Very high	5
		6 – 14	High	4
		14 – 21	Moderate	3
		21 – 31	Low	2
		31 – 72	Very low	1
2	Elevation	0 – 140	Very high	5
		140 – 313	High	4
		313 – 507	Moderate	3
		507 – 702	Low	2
		702 – 1033	Very low	1
3	Rainfall	604 – 613	Very low	1
		613- 621	Low	2
		621 – 630	Moderate	3
		630 – 636	High	4
		636 - 643	Very high	5
4	LULC	Water	High	4
		Trees	Very low	1
		Crops	Low	2
		Building Area	Very high	5
		Bare Land	Moderate	3
		Range Land	Moderate	3
5	Distance from river	0 – 500	Very high	5
		500 – 1000	High	4
		1000 – 1500	Moderate	3
		1500 – 2000	Low	2
		2000 – 3 936,98	Very low	1
6	Drainage density	0 – 0.63	Very low	1
		0.63 – 1.62	Low	2
		1.62 – 1.89	Moderate	3
		1.89 – 2.52	High	4
		2.52 – 3.15	Very high	5
7	Topographic wetness index	0 – 2	Very low	1
		2 – 3.26	Low	2
		3.26 – 5.36	Moderate	3
		5.36 – 8.54	High	4
		8.54 – 12.17	Very high	5

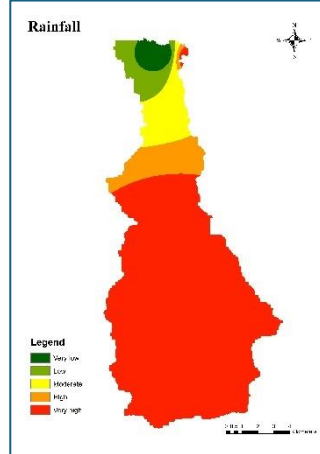
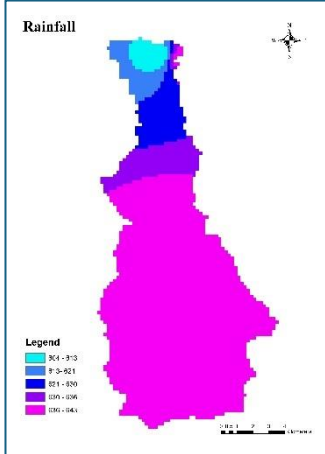
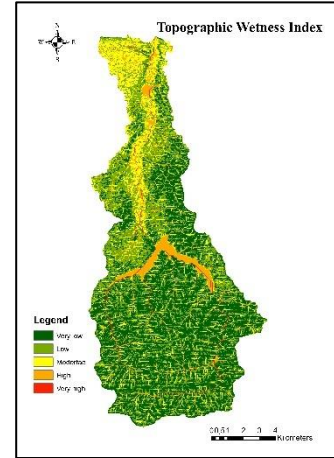
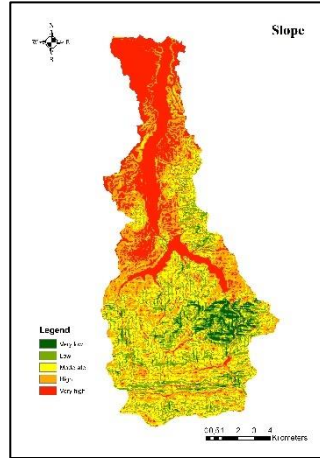
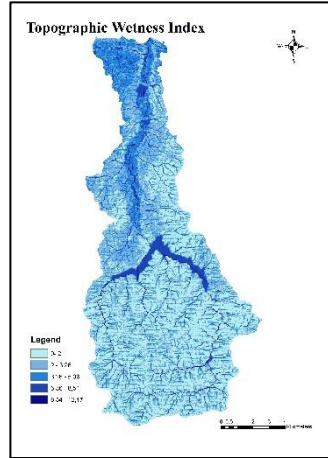
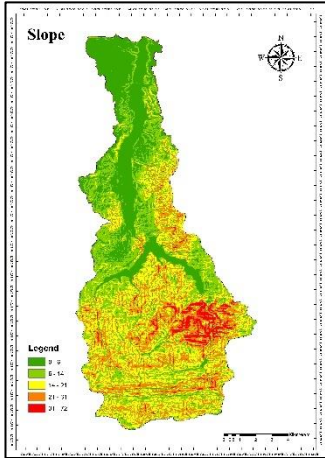
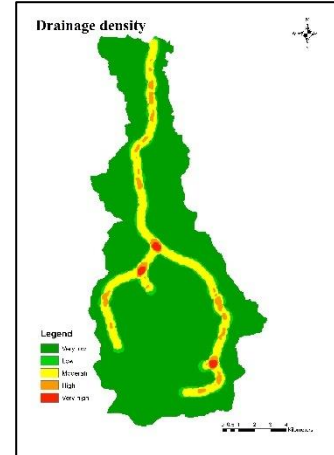
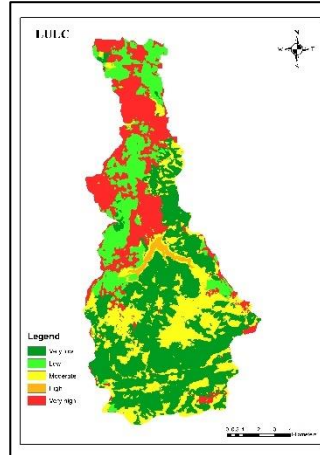
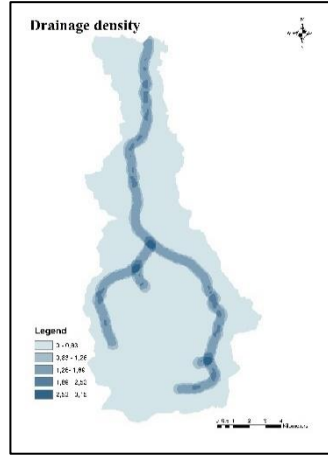
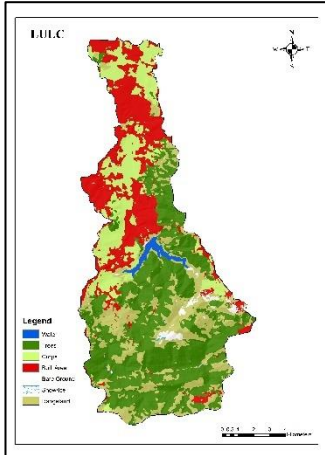
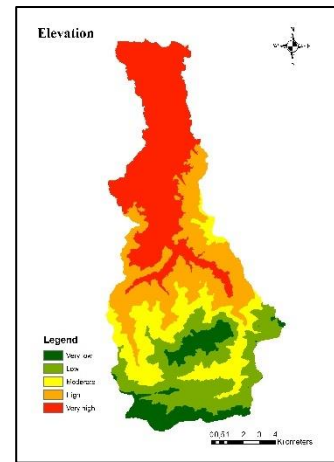
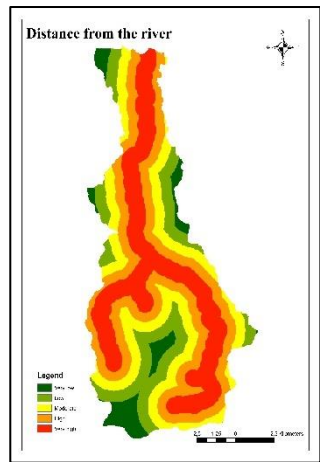
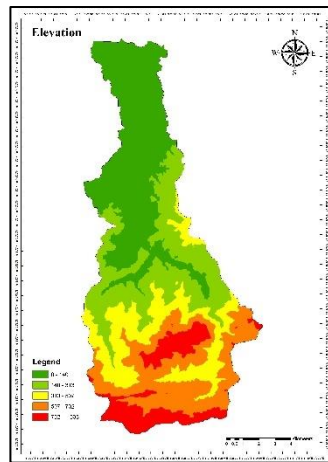
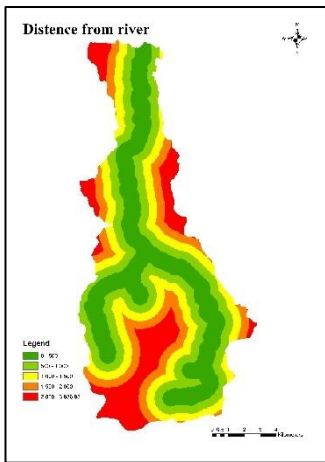


**Figure 13: Factors classification.**

Based on Figure 14, the final flood vulnerability map of the Boudouaou watershed was created by integrating seven thematic layers that represent various flood factors (Figure 15).

The map clearly illustrates spatial variations in vulnerability, classified into five distinct categories: very low, low, moderate, high, and very high. Analysis of the map shows that the areas situated proximity to the main Wadi Boudouaou exhibit from very high to high vulnerability to flooding incidents compared to other parts of the basin. Low elevation and comparatively flat slopes, high drainage density, heavy rainfall, high drainage density, high topographic wetness index (TWI), and substantial urbanization in close proximity to the wadi are the characteristics that define these areas.

Conversely, the peripheral parts of the watershed, particularly along the southern boundary, generally have low to very low levels of vulnerability. Such areas are generally characterized by higher altitudes, lower drainage densities, and more favorable land cover patterns with high vegetation cover that promote water infiltration and consequently reduce flood potential.

According to the findings, the areas of Kharouba Ouled ben shettakh, boudouaou, Harrachi, Ben yamina, and ben marzouga have been identified as the most vulnerable to flooding.

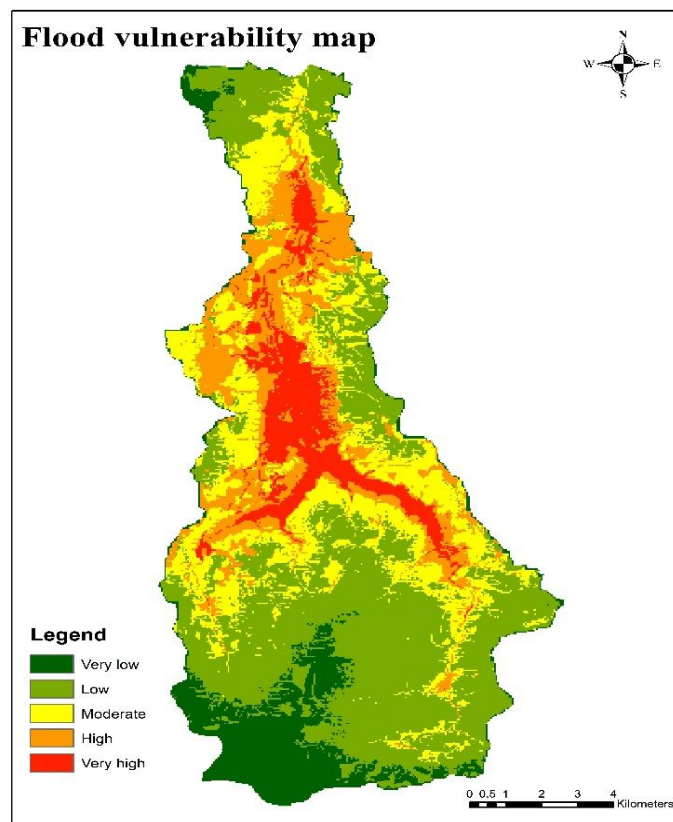


**Figure 14: Flood vulnerability map.**

## **Part 02: Flood Hazard Mapping using the RRI Model**

### **4.2.1 Introduction**

In this study section, the RRI model was employed to calculate the flood hazard in the study area considering two major scenarios: with existing dam infrastructure and without the dam. In order to assess the complete effect of various rainfall intensities on the characteristics of a flood, model simulations for four various rainfall scenarios have been conducted: the actual rainfall event (historical data) and hypothetical cases for an increase of 20%, 60%, and 100% compared to the actual event.

### **4.2.2 Model Calibration and Validation**

Calibration is an essential process to achieve accurate and trustworthy results from flood simulation. However, due to the complexity and high computational demand of the Rainfall-Runoff-Inundation (RRI) model, each simulation consumes a considerable amount of time, the present simulations utilized input parameters of a previous Algerian study where the RRI model demonstrated good performance and strong correlation with observed data for our study. The performance of the RRI model was evaluated using two generally accepted statistical metrics: the Nash–Sutcliffe Efficiency (ENS) and the Coefficient of Determination ( $R^2$ ). The results from the chosen calibration parameters indicated a good performance of the model with a Nash–Sutcliffe efficiency (ENS) of 0.72 and a Coefficient of Determination ( $R^2$ ) of 0.75. These values demonstrate a high correlation and good accuracy between simulated flooding conditions and observed data, justifying the fact that input parameters from the former Algerian research are optimal and reliable for the current simulations.

### **4.2.3 Simulation Scenarios and Setup**

To assess flood hazards in the entire watershed comprehensively, the model was employed under two basic hydraulic management conditions: without the dam (natural condition) and with the dam (accounting for the maximum dam outflow between 1993 and 2024). For both conditions, four different rainfall conditions were analyzed: the real rain event and three hypothetical cases representing increased rainfall intensities by 20%, 60%, and 100% over the real event.

#### 4.2.3.1 Scenarios 1: without the Dam and with the dam

##### a) Without the dam scenario (Actual rainfall event)

The flood hazard map is evidently delineating high flood danger areas that are predominantly located along river channels and surrounding lowland zones. Urban and cultivated areas immediately abutting river channels are inherently more susceptible to flooding because they are within floodplains, justifying the need for targeted risk reduction measures applied to these critical zones.

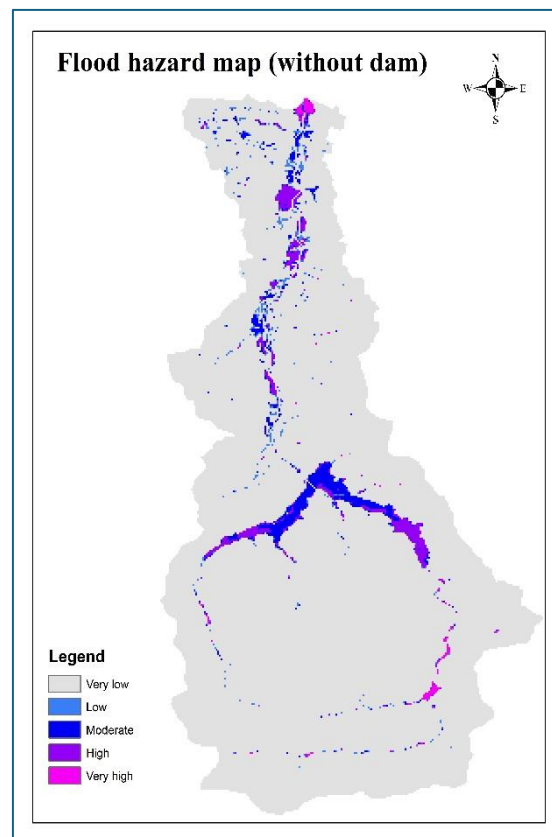


**Figure 4.3:** Flood Hazard Map (Without the dam) under Actual Rainfall Conditions.

##### b) With the dam scenarios (Maximum Dam Outflow)

In this scenario, the flood risk was simulated under the actual rainfall event, including the peak outflow discharge from the dam.

The flood hazard map for this scenario represents the spatial pattern of flood risk in the watershed under the real rainfall event with the presence of Keddara Dam. As can be observed from the map, the most vulnerable areas remain those directly next to river channels and low-lying regions, emphasizing the need for localized flood protection in those regions.

The map classifies flood hazard into five classes: very low, low, moderate, high, and very high. The high-to-very-high hazard zones are clearly visible mostly in the central and northern parts of the watershed, particularly in the downstream area. These zones are closely correlated with low-lying areas and natural drainage paths, suggesting that topography remains the main determinant of flood exposure in the Boudouaou watershed.

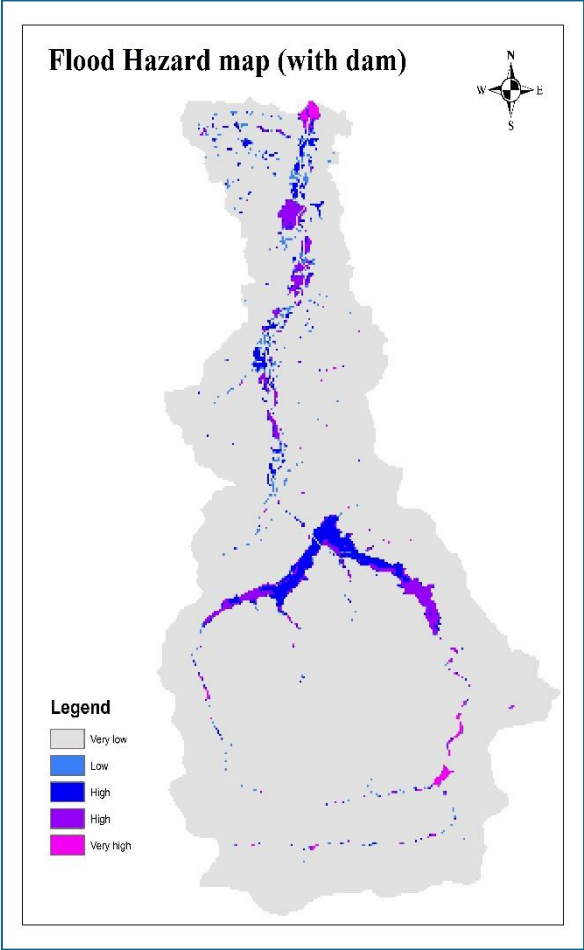


**Figure 4.3:** Flood Hazard Map (With the dam) under Actual Rainfall Conditions.

**4.2.3.2 Comparative Analysis of Scenarios**

Comparing the flood hazard maps for the two Scenario with dam Scenario without dam under one and the same actual rainfall event, it is apparent that the variation between flood extent and intensity is extremely small and nearly negligible.

Although the simulation case was computed using the dam's highest outflow value of 4.3 m<sup>3</sup>/s, examining more closely 1993–2024 historical outflow recordings reveal well over 95% of the time the measured outflow was a value of 0 m<sup>3</sup>/s. This indicates the dam is infrequently used to supply water to the downstream river system. Furthermore, authoritative information from ANBT (National Agency for Dams and Transfers) confirms that the dam is designed to meet

the drinking water needs of the Algiers metropolitan area, pointing towards its functioning being directed towards water conservation and storage rather than flood regulation.

On this point, the maximum outflow value used during simulation may not always be an emergency spillway or maximum storage level response. Instead, it will probably be an operating capacity for water supply or transfer. Furthermore, since the dam is continuously providing water for domestic consumption, its water levels are continuously being drawn down, reducing the chances of spillover or uncontrolled release under normal rainfall conditions.

Therefore, the minor variation that was registered between the "with the dam" and "without the dam" flood hazard conditions can be explained by the fact that, in real operational conditions, the dam is not currently generating extra flooding within the watershed.

### **c) Increased Rainfall Conditions scenario (20%, 60%, 100%)**

With a further 20% increase in rainfall, we encounter the high and very high-hazard zones moderately expanding, particularly that of the main course and tributaries of the river. Weak areas, primarily urbanized and arable land along the riverbanks, already bear testimony to increased exposure at this 20% increase in rainfall. At an increase of 60% in rainfall, the hazard becomes more pronounced. The very high hazard regions expand considerably, covering more of the floodplain and extending into previously low- or moderate-risk areas. This shows much higher rates of surface runoff and water storage, overloading natural drainage systems and increasing the threat of catastrophic downstream flooding. The 100% rainfall increase scenario flood hazard map (simulating the impact of a doubling of rainfall intensity over the 10-day period) illustrates a dramatic expansion of high and very high hazard areas, particularly along the main river channels and low-lying sections of the floodplains. The central and southern portions of the basin are especially affected, with extremely high hazard zones forming continuous, large patches, suggesting deep inundation and high velocities of flow.

The simulation points to the vulnerability of the watershed to extreme climate events under the absence of flood regulation infrastructure, emphasizing the pressing need for proactive flood risk management measures.

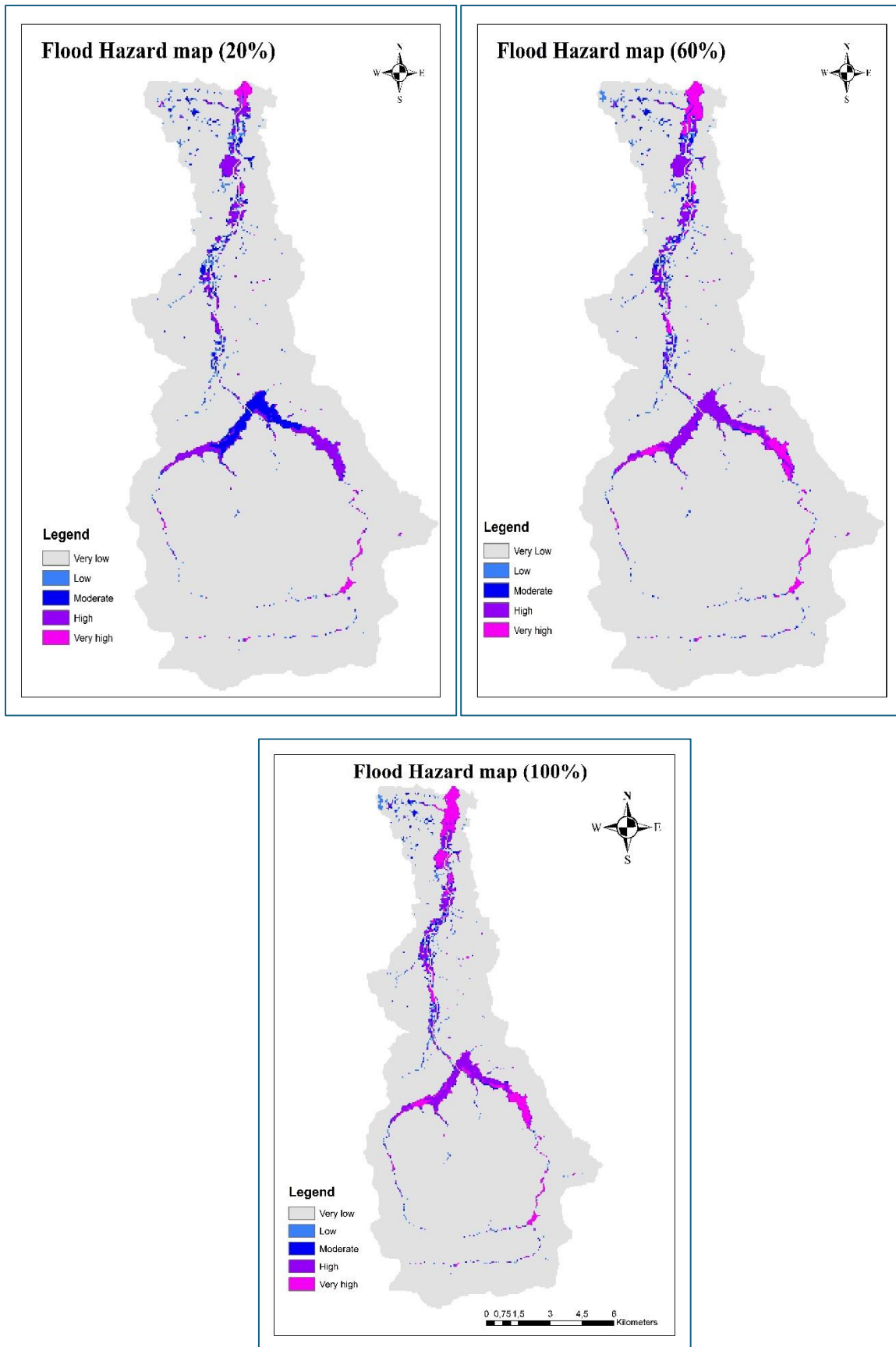


**Figure 15:** Hazard Maps Under Increased Rainfall Scenarios (Without Dam: +20%, +60%, +100%).

## **Part 03: Flood risk mapping**

### **4.3.1 Introduction**

Flood risk is a function of both flood hazard and flood vulnerability. While flood hazard is the probability and intensity of flooding in a region, vulnerability is the susceptibility of a region's population, infrastructure, and land use to be impacted. Flood risk in this study is approximated by overlaying the results of the RRI model simulations (hazard) and the AHP-based vulnerability mapping in a GIS-based overlay approach. The combination of these elements enables a spatial determination of zones most vulnerable for various levels of rainfall.

### **4.3.2 Flood Risk Maps and Interpretation**

#### **A. Actual rainfall event scenario**

The flood risk map generated under the actual rainfall event scenario (Figure 17) provides a spatial distribution of zones under various degrees of flood risk. The resulting classification ranges between very low and very high flood risk. The very high-risk zones are generally concentrated along the main river channels, particularly in the central and southern portions of the watershed. These areas overlap with low-lying floodplains, which are characterized by high flow accumulation and moderate-to-high susceptibility due to proximity to rivers, land use (croplands and built-up areas), and lower elevations. Medium and high-risk areas extend from the riverbanks and into the transitions, often blanketing fields, rural settlements, and infrastructure corridors. These areas are susceptible to overbank inundation and surface runoff accumulation during prolonged rainfall.

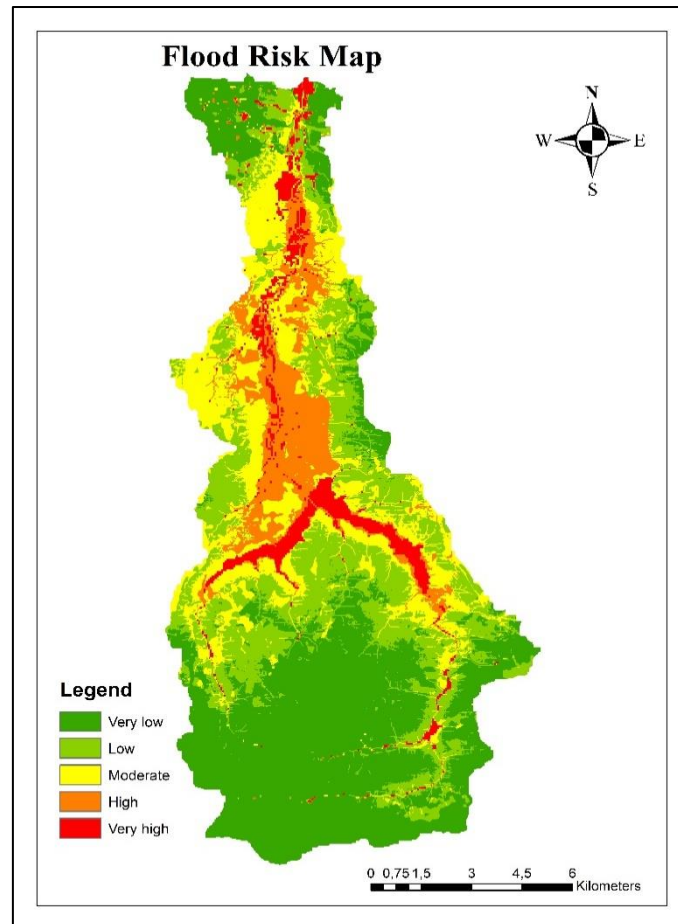


**Figure 16:** Flood Risk map.

### **B. Increased Rainfall Conditions scenario (20%, 60%, 100%)**

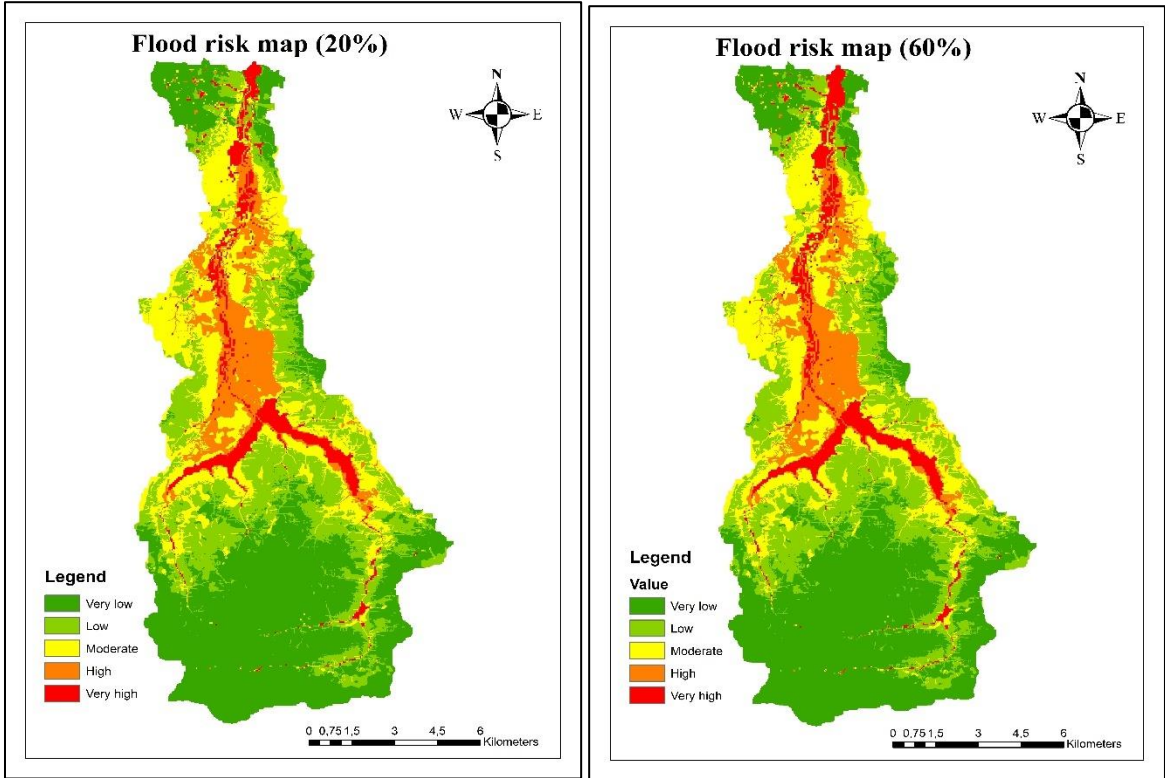
The maps of flood risk displayed in Figure 18 represent the spatial variation of flood risk in three climatic change scenarios of rainfall increase, namely +20%, +60%, and +100%. The patterns exhibit an overall trend towards more severity and extent of flood risk with elevated rainfall intensity, emphasizing the master control role played by future climatic change on flood behavior within the watershed.

For the +20% case, the risk of floods increases compared to the actual event of rainfall. Very high- and high-risk classes begin growing much more predominantly in major river courses and flood plains, particularly within the northern and central sections of the basin. While much of the southern region remains within low and very low-risk classes.

The +60% scenario forecasts a spectacular upsurge of flood risk. The high-risk areas increase in size and become more connected, forming unbroken corridors along rivers. The emergence of moderate-risk areas into new low-risk domains implies an increase in the susceptibility of

infrastructure, croplands, and roads to flood threat. This quantity of rainfall represents a severe livelihood and land-use threat.

In the +100% case, flood hazard is extensive and severe. Very high-risk zones dominate the main valleys and extend far into tributary areas, involving huge swathes of urban and farmland. The overall pattern indicates that the watershed hydrological capacity is exceeded, and most of the floodplain is in the high and very high-risk category, which exhibits the susceptibility of the watershed and the urgent need for resilient flood management planning.



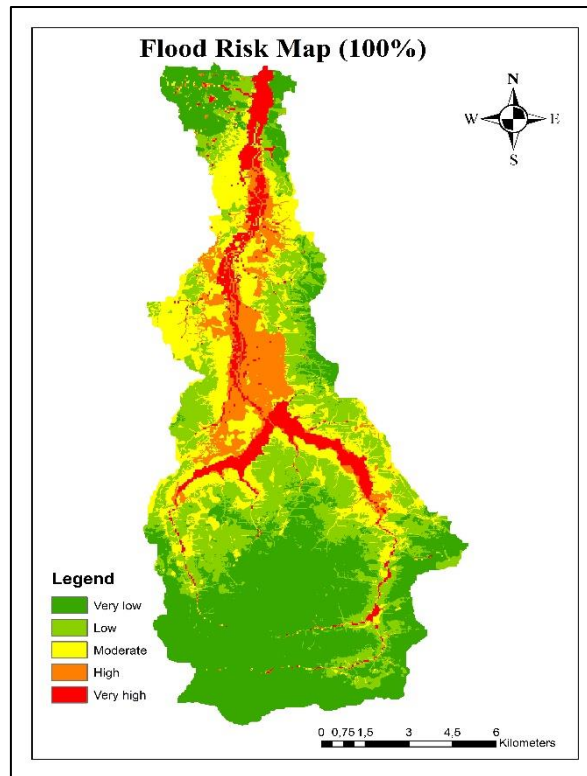


**Figure 17:** Flood Risk Maps Under Increased Rainfall Conditions (20%, 60%, 100%).

### 4.3.3 Proposed Flood Risk Management Solutions

#### 1. Construction of Small Retention Basins

Japan has used flooded sports facilities such as tennis courts as part of its urban flood management strategy, particularly in densely populated cities like Tokyo. In Algeria, especially in the Wadi Boudouaou basin we can use the football courts as a retention basin. Many Algerian cities and villages have football fields or school playgrounds near populated zones that are already flood prone.

#### 2. Flood Early Warning Systems

EWS is critical for reducing casualties and economic losses, such as Developing SMS/voice alerts via mobile networks for vulnerable communities. Furthermore, installing low-cost sensors or partner with national weather services for real-time alerts.

#### 3. Reinforcement of Riverbanks

Using gabions, levees, or revetments to protect high-risk areas along the central river corridor especially in the very high-risk zones.

#### 1. Community Awareness and Capacity Building

Conduct training in vulnerable areas on flood response, evacuation, and preparedness.

**5**

---

**CONCLUSION**

## CHAPTER FIVE: CONCLUSION

### 6.1 Conclusion

This study assessed flood risk in the Wadi Boudouaou watershed of northern Algeria by integrating spatial flood vulnerability analysis and hydrological flood hazard simulation. The Analytic Hierarchy Process (AHP) was applied using six principal factors—elevation, slope, rainfall, drainage density, distance from rivers, and the topographic wetness index (TWI)—to generate a flood vulnerability map. Simultaneously, the Rainfall-Runoff-Inundation (RRI) model was used to simulate flood hazard for two dam-scenario conditions (with and without Keddara Dam) and under various rainfall intensities (real event, +20%, +60%, and +100%), which correspond to possible future climate conditions.

The calibration of the RRI model using validated parameters from a previous Algerian study conducted well, with Nash–Sutcliffe Efficiency of 0.72 and  $R^2$  of 0.75. The flood hazard maps derived showed that the severity and extent of floods increased significantly with higher rainfall scenarios, particularly in low-lying parts of the floodplains near the river channels.

Unexpectedly, the presence of the Keddara Dam showed small differences in flood hazard, largely due to its operating priority for domestic water supply and since more than 95% of outflow records contained 0 m<sup>3</sup>/s for the last three decades. It confirms that the dam does not play any significant role in the increasing of floods under normal or even extraordinary rain events.

The flood risk maps produced by overlaying the hazard and vulnerability information revealed several very high-risk locations, especially along river courses and in agricultural or urbanized areas. The maps represent a valuable tool for identifying areas where flood mitigation and preparedness interventions should be prioritized.

---

**REFERENCES**

## CHAPTER SIX: REFERENCES

Ziadi, S., & Keraghel, M. A. (2023). Flooding vulnerability in Algiers (Algeria): An Analytic Hierarchy Process. Research Square (Research Square). <https://doi.org/10.21203/rs.3.rs-2648607/v1>

Kundzewicz, Z. W., Su, B., Wang, Y., Wang, G., Wang, G., Huang, J., & Jiang, T. (2019). Flood risk in a range of spatial perspectives – from global to local scales. *Natural Hazards and Earth System Sciences*, 19(7), 1319–1328. <https://doi.org/10.5194/nhess-19-1319-2019>

Merz, B., Blöschl, G., Vorogushyn, S. et al. Causes, impacts and patterns of disastrous river floods. *Nat Rev Earth Environ* 2, 592–609 (2021). <https://doi.org/10.1038/s43017-021-00195-3>

Zhang, P., Sun, W., Xiao, P., Yao, W., & Liu, G. (2022). Driving factors of heavy rainfall causing flash floods in the middle reaches of the Yellow River: a case study in the Wuding River basin, China. *Sustainability*, 14(13), 8004. <https://doi.org/10.3390/su14138004>

Hassan, B. T., Yassine, M., & Amin, D. (2022). Comparison of urbanization, climate change, and drainage design impacts on urban flashfloods in an arid region: case study, New Cairo, Egypt. *Water*, 14(15), 2430. <https://doi.org/10.3390/w14152430>

Douglas, I., Alam, K., Maghenda, M., McDonnell, Y., Mclean, L., & Campbell, J. (2008). Unjust waters: climate change, flooding and the urban poor in Africa. *Environment & Urbanization*, 20(1), 187-205. <https://doi.org/10.1177/0956247808089156>

Zekouda, N. N., Meddi, M., LaVanchy, G. T., & Remaoun, M. (2020). The impact of human activities on flood trends in the Semi-Arid Climate of Cheliff Basin, Algeria. *Water Resources*, 47(3), 409–420. <https://doi.org/10.1134/s0097807820030136>

Abdrabo, K. I., Kantosh, S. A., Saber, M., Sumi, T., Elleithy, D., Habiba, O. M., & Alboshy, B. (2021). The role of urban planning and landscape tools concerning flash flood risk reduction within arid and semiarid regions. In *Natural disaster science and mitigation engineering: DPRI reports* (pp. 283–316). [https://doi.org/10.1007/978-981-16-2904-4\\_11](https://doi.org/10.1007/978-981-16-2904-4_11)

Taib, L. (2024). Flood risk assessment for better city resilience; case of the Bab el Oued agglomeration, Algiers (Algeria). *Indonesian Journal of Social Science Research*, 5(1), 149–165. <https://doi.org/10.11594/ijssr.05.01.14>

Aldardasawi, A. F. M., & Eren, B. (2021). Floods and their impact on the environment. *Academic Perspective Procedia*, 4(2), 42–49. <https://doi.org/10.33793/acperpro.04.02.24>

Breinl, K., Lun, D., Müller-Thomy, H., & Blöschl, G. (2021). Understanding the relationship between rainfall and flood probabilities through combined intensity-duration-frequency analysis. *Journal of Hydrology*, 602, 126759. <https://doi.org/10.1016/j.jhydrol.2021.126759>

Hasanuzzaman, M., Adhikary, P. P., Bera, B., & Shit, P. K. (2022). Flood vulnerability assessment using AHP and frequency ratio techniques. In *Springer eBooks* (pp. 91–104). [https://doi.org/10.1007/978-3-030-94544-2\\_6](https://doi.org/10.1007/978-3-030-94544-2_6)

Ahmed, I., Das, N., Debnath, J., Bhowmik, M., & Bhattacharjee, S. (2023b). Flood hazard zonation using GIS-based multi-parametric Analytical Hierarchy Process. <https://www.semanticscholar.org/paper/Flood-hazard-zonation-using-GIS-based-Analytical-Ahmed-Das/b2ff81038ebd6f490c1c2785c9d08d7ace448c59>

Vignesh, K. S., Anandakumar, I., Ranjan, R., & Borah, D. (2020c). Flood vulnerability assessment using an integrated approach of multi-criteria decision-making model and geospatial techniques. *Modeling Earth Systems and Environment*, 7(2), 767–781. <https://doi.org/10.1007/s40808-020-00997-2>

Khoeun, C., Sok, T., Chan, R., Khe, S., Ich, I., Chan, K., & Oeurng, C. (2022b). Assessing Flood Hazard Index using Analytical Hierarchy Process (AHP) and Geographical Information System (GIS) in Stung Sen River Basin. *IOP Conference Series Earth and Environmental Science*, 1091(1), 012031. <https://doi.org/10.1088/1755-1315/1091/1/012031>

Koem, C., & Tantanee, S. (2020). Flash flood hazard mapping based on AHP with GIS and satellite information in Kampong Speu Province, Cambodia. *International Journal of Disaster Resilience in the Built Environment*, 12(5), 457–470. <https://doi.org/10.1108/ijdrbe-09-2020-0099>

Ouma, Y., & Tateishi, R. (2014). Urban flood vulnerability and risk mapping using integrated multi-parametric AHP and GIS methodological overview and case study assessment. *Water*, 6(6), 1515–1545. <https://doi.org/10.3390/w6061515>

Feloni, E., Mousadis, I., & Baltas, E. (2019). Flood vulnerability assessment using a GIS-based multi-criteria approach—The case of Attica region. *Journal of Flood Risk Management*, 13(S1). <https://doi.org/10.1111/jfr3.12563>

Sharir, K., Goh, T., Simon, N., Lee, K. E., Talip, M., & Roslee, R. (2022). Assessment of flood susceptibility analysis using Analytical Hierarchy Process (AHP) in Kota Belud area, Sabah, Malaysia. *IOP Conference Series: Earth and Environmental Science*, 1103(1), 012005. <https://doi.org/10.1088/1755-1315/1103/1/012005>

Swain, K. C., Singha, C., & Nayak, L. (2020b). Flood Susceptibility Mapping through the GIS-AHP Technique Using the Cloud. *ISPRS International Journal of Geo-Information*, 9(12), 720. <https://doi.org/10.3390/ijgi9120720>

Koroma, A. O., Saber, M., & Abdelbaki, C. (2024). Urban Flood Vulnerability Assessment in Freetown, Sierra Leone: AHP approach. *Hydrology*, 11(10), 158. <https://doi.org/10.3390/hydrology11100158>

Seejata, K., Yodying, A., Wongthadam, T., Mahavik, N., & Tantanee, S. (2018b). Assessment of flood hazard areas using Analytical Hierarchy Process over the Lower Yom Basin, Sukhothai Province. *Procedia Engineering*, 212, 340–347. <https://doi.org/10.1016/j.proeng.2018.01.044>

Kazakis, N., Kougiyas, I., & Patsialis, T. (2015). Assessment of flood hazard areas at a regional scale using an index-based approach and Analytical Hierarchy Process: Application in Rhodope–Evros region, Greece. *The Science of the Total Environment*, 538, 555–563. <https://doi.org/10.1016/j.scitotenv.2015.08.055>

Vignesh, K. S., Anandakumar, I., Ranjan, R., & Borah, D. (2020b). Flood vulnerability assessment using an integrated approach of multi-criteria decision-making model and geospatial techniques. *Modeling Earth Systems and Environment*, 7(2), 767–781. <https://doi.org/10.1007/s40808-020-00997-2>

Rebouh, N., Tout, F., Dinar, H., Benzid, Y., & Zouak, Z. (2024b). Integrating Multi-Source geospatial data and AHP for flood susceptibility mapping in Ain Smara, Constantine, Algeria. *International Journal of Disaster Risk Management*, 6(2), 245–263. <https://doi.org/10.18485/ijdrm.2024.6.2.16>

Hammami, S., Zouhri, L., Souissi, D., Souei, A., Zghibi, A., Marzougui, A., & Dlala, M. (2019). Application of the GIS based multi-criteria decision analysis and analytical hierarchy

process (AHP) in the flood susceptibility mapping (Tunisia). *Arabian Journal of Geosciences*, 12(21). <https://doi.org/10.1007/s12517-019-4754-9>

Dandapat, K., & Panda, G. K. (2017). Flood vulnerability analysis and risk assessment using analytical hierarchy process. *Modeling Earth Systems and Environment*, 3(4), 1627–1646. <https://doi.org/10.1007/s40808-017-0388-7>

Abdessamed, D., & Abderrazak, B. (2019). Coupling HEC-RAS and HEC-HMS in rainfall–runoff modeling and evaluating floodplain inundation maps in arid environments: case study of Ain Sefra city, Ksour Mountain. SW of Algeria. *Environmental Earth Sciences*, 78(19). <https://doi.org/10.1007/s12665-019-8604-6>

Abdrabo, K. I., Kantoush, S. A., Saber, M., Sumi, T., Habiba, O. M., Elleithy, D., & Elboshy, B. (2020). Integrated Methodology for urban flood risk mapping at the microscale in ungauged Regions: A case study of Hurghada, Egypt. *Remote Sensing*, 12(21), 3548. <https://doi.org/10.3390/rs12213548>

Afra, A., Berrezel, Y. A., Abdelbaki, C., Megnounif, A., Saber, M., Benabdelkrim, M. E. A., & Kumar, N. (2025). Application of the Rainfall–Runoff–Inundation model for flood risk assessment in the Mekerra Basin, Algeria. *GeoHazards*, 6(1), 2. <https://doi.org/10.3390/geohazards6010002>

Ahmed, I., Das, N., Debnath, J., Bhowmik, M., & Bhattacharjee, S. (2023). Flood hazard zonation using GIS-based multi-parametric Analytical Hierarchy Process. *Geosystems and Geoenvironment*, 3(2), 100250. <https://doi.org/10.1016/j.geogeo.2023.100250>

Aichi, A., Ikirri, M., Mohamed, A. H., Quesada-Román, A., Sahoo, S., Singha, C., Sajinkumar, K. S., Abioui, M., & Quesada-Román, A. (2024). Integrated GIS and Analytic Hierarchy Process for flood risk assessment in the Dades Wadi watershed (Central High Atlas, Morocco). *Results in Earth Sciences*. <https://doi.org/10.1016/j.rines.2024.100019>

Ali, K., Bajracharya, R. M., & Koirala, H. L. (2016). A review of flood risk assessment. *Neliti*. <https://www.neliti.com/publications/238636/a-review-of-flood-risk-assessment>

Almouctar, M. a. S., Wu, Y., An, S., Yin, X., Qin, C., Zhao, F., & Qiu, L. (2024b). Flood risk assessment in arid and semi-arid regions using Multi-criteria approaches and remote sensing in a data-scarce region. *Journal of Hydrology Regional Studies*, 54, 101862. <https://doi.org/10.1016/j.ejrh.2024.101862>

An, T. T., Izuru, S., Narumasa, T., Raghavan, V., Hanh, L. N., Van An, N., Long, N. V., Thuy, N. T., & Minh, T. P. (2022). Flood vulnerability assessment at the local scale using remote sensing and GIS techniques: a case study in Da Nang City, Vietnam. *Journal of Water and Climate Change*, 13(9), 3217–3238. <https://doi.org/10.2166/wcc.2022.029>

Astite, S. W., Medjerab, A., Belabid, N., Mahmoudi, N. E., Wartiti, M. E., & Kemmou, S. (2015). Cartography of flood hazard by overflowing rivers using hydraulic modeling and geographic information system: Oued El Harrach case (North of Algeria). *Revista De Teledetección*, 44, 67. <https://doi.org/10.4995/raet.2015.3985>

Aydin, M. C., & Birincioğlu, E. S. (2022). Flood risk analysis using gis-based analytical hierarchy process: a case study of Bitlis Province. *Applied Water Science*, 12(6). <https://doi.org/10.1007/s13201-022-01655-x>

Aynew, W., & Kebede, H. (2023). GIS and remote sensing based flood risk assessment and mapping: The case of Dikala Watershed in Kobo Woreda Amhara Region, Ethiopia. *Environmental and Sustainability Indicators*.

Baalousha, H. M., Younes, A., Yassin, M. A., & Fahs, M. (2023). Comparison of the Fuzzy Analytic Hierarchy Process (F-AHP) and fuzzy logic for flood exposure risk assessment in arid regions. *Hydrology*, 10(7), 136. <https://doi.org/10.3390/hydrology10070136>

Bekhira, A., Habi, M., & Morsli, B. (2019). Management of hazard of flooding in arid region urban agglomeration using HEC-RAS and GIS software: The case of the Bechar's city. *Journal of Water and Land Development*, 42(1), 21–32. <https://doi.org/10.2478/jwld-2019-0041>

Belazreg, N. E. H., Hasbaia, M., Şen, Z., & Ferhati, A. (2023). Flood risk mapping using multi-criteria analysis (MCA) through AHP method case of El-Ham wadi watershed of Hodna basin (Algeria). *Natural Hazards*, 120(2), 1023–1039. <https://doi.org/10.1007/s11069-023-06239-9>

Bhagabati, S. S., & Kawasaki, A. (2017). Consideration of the rainfall-runoff-inundation (RRI) model for flood mapping in a deltaic area of Myanmar. *Hydrological Research Letters*, 11(3), 155–160. <https://doi.org/10.3178/hrl.11.15>

Bhatt, G., Sinha, K., Deka, P., & Kumar, A. (2014). Flood hazard and risk assessment in Chamoli District, Uttarakhand using Satellite Remote sensing and GIS techniques. <https://www.semanticscholar.org/paper/Flood-Hazard-and-Risk-Assessment-in-Chamoli-Using-Bhatt-Sinha/0e94c417dbd28d7c4750769c78ec560f14c2beb1>

Boulaghmen, F., Benouar, D., & Kalbaza, M. (2018). Management of flood risk in the center of Ghardaia city with a geographic information system (SIG) after the flashflood of 1st October 2008. <https://www.semanticscholar.org/paper/Management-of-flood-risk-in-the-center-of-Ghardaia-Boulaghmen-Benouar/591ebf1048066dc4a5547aea549f60e2977d2f47>

Boutaghane, H., Boulmaiz, T., Lameche, E. K., Lefkir, A., Hasbaia, M., Abdelbaki, C., Moulahoum, A. W., Keblouti, M., & Bermad, A. (2021). Flood analysis and mitigation strategies in Algeria. In *Natural disaster science and mitigation engineering: DPR I reports* (pp. 95–118). [https://doi.org/10.1007/978-981-16-2904-4\\_3](https://doi.org/10.1007/978-981-16-2904-4_3)

Chan, S. W., Abid, S. K., Sulaiman, N., Nazir, U., & Azam, K. (2022). A systematic review of the flood vulnerability using geographic information system. *Heliyon*, 8(3), e09075. <https://doi.org/10.1016/j.heliyon.2022.e09075>

Chung, S., Takeuchi, J., Fujihara, M., & Oeurng, C. (2019). Flood damage assessment on rice crop in the Stung Sen River Basin of Cambodia. *Paddy and Water Environment*, 17(2), 255–263. <https://doi.org/10.1007/s10333-019-00718-1>

De Brito, M. M., Evers, M., & Almoradie, A. D. S. (2018). Participatory flood vulnerability assessment: a multi-criteria approach. *Hydrology and Earth System Sciences*, 22(1), 373–390. <https://doi.org/10.5194/hess-22-373-2018>

Deb, P., & Kiem, A. S. (2020). Evaluation of rainfall–runoff model performance under non-stationary hydroclimatic conditions. *Hydrological Sciences Journal*, 65(10), 1667–1684. <https://doi.org/10.1080/02626667.2020.1754420>

Diriba, D., Takele, T., Karuppanan, S., & Husein, M. (2024b). Flood hazard analysis and risk assessment using remote sensing, GIS, and AHP techniques: a case study of the Gidabo Watershed, main Ethiopian Rift, Ethiopia. *Geomatics Natural Hazards and Risk*, 15(1). <https://doi.org/10.1080/19475705.2024.236181>

Edamo, M. L., Ukumo, T. Y., Lohani, T. K., Mirani, K. B., & Ayele, M. A. (2022). Flood inundation mapping under climate change scenarios in the Boyo watershed of Southern Ethiopia. *Journal of Water and Climate Change*, 13(8), 3170–3188. <https://doi.org/10.2166/wcc.2022.193>

Elsebaie, I. H., Kawara, A. Q., & Alnahit, A. O. (2023). Mapping and assessment of flood risk in the Wadi Al-Lith Basin, Saudi Arabia. *Water*, 15(5), 902. <https://doi.org/10.3390/w15050902>

Gashaw, W., & Legesse, D. (2011). Flood hazard and risk assessment using GIS and remote sensing in Fogera Woreda, northwest Ethiopia. In Springer eBooks (pp. 179–206). [https://doi.org/10.1007/978-94-007-0689-7\\_9](https://doi.org/10.1007/978-94-007-0689-7_9)

Gholami, V., & Khaleghi, M. R. (2021). A simulation of the rainfall-runoff process using artificial neural network and HEC-HMS model in forest lands. *Journal of Forest Science*, 67(4), 165–174. <https://doi.org/10.17221/90/2020-jfs>

Ghosh, A., Chatterjee, U., Pal, S. C., Islam, A. R. M. T., Alam, E., & Islam, M. K. (2023). Flood hazard mapping using GIS-based statistical model in vulnerable riparian regions of subtropical environment. *Geocarto International*, 38(1). <https://doi.org/10.1080/10106049.2023.2285355>

Glago, F. J. (2021). Flood Disaster Hazards; Causes, Impacts and Management: A State-of-the-Art Review. IntechOpen eBooks. <https://doi.org/10.5772/intechopen.95048>

Grigg, N. S. (2023b). Comprehensive Flood Risk Assessment: state of the practice. *Hydrology*, 10(2), 46. <https://doi.org/10.3390/hydrology1002004>

Hagos, Y. G., Andualem, T. G., Yibeltal, M., & Mengie, M. A. (2022). Flood hazard assessment and mapping using GIS integrated with multi-criteria decision analysis in upper Awash River basin, Ethiopia. *Applied Water Science*, 12(7). <https://doi.org/10.1007/s13201-022-01674-8>

Hanan, N. a. M., Abas, M. A., Nor, A. N. M., Amin, M. F. M., Hassin, N. H., Yusoff, A. H., Awang, N. R., Mohamed, S., & Wee, S. T. (2020). A GIS-Based flood vulnerability assessment in Pasir Mas, Kelantan. *IOP Conference Series Earth and Environmental Science*, 549(1), 012004. <https://doi.org/10.1088/1755-1315/549/1/012004>

Hassani, F. E., Hattafi, Y., & Lahrach, A. (2021). Water dynamics of the Sefrou Watershed, Northern Tabular Middle Atlas, Morocco. *Journal of Geoscience and Environment Protection*, 09(09), 102–130. <https://doi.org/10.4236/gep.2021.99007>

Helmi, A. M., & Zohny, O. (2020). Flash flood risk assessment in Egypt. In *Advances in Science, Technology & Innovation/Advances in science, technology & innovation* (pp. 253–312). [https://doi.org/10.1007/978-3-030-29635-3\\_13](https://doi.org/10.1007/978-3-030-29635-3_13)

Ibrahim, O. A., Goshime, D. W., Tekleab, S., & Absi, R. (2023). Flood Inundation mapping and mitigation options in data-scarce region of Beledwayne town in the Wabi Shebele River

Basin of Somalia. *Natural Hazards Research*, 4(2), 336–346.  
<https://doi.org/10.1016/j.nhres.2023.11.001>

Ikhwali, M. F., Azhari, B., Khari, A., Nur, S., Hamdan, A. M., & Prommacot, K. (2023). The application and relevancy of Rainfall-Runoff-Inundation (RRI) model in Indonesia. *Elkawnie*, 9(1), 111. <https://doi.org/10.22373/ekw.v9i1.14577>

International Bank for Reconstruction and Development/World Bank. (2016). *Methods in flood hazard and risk assessment: CAPRA—Technical notes*. Washington, DC: World Bank.

Ishizaka, A., & Labib, A. (2011). Review of the main developments in the analytic hierarchy process. *Expert Systems with Applications*, 38, 14336-14345.  
<https://doi.org/10.1016/j.eswa.2011.04.143>

Jehanzaib, M., Ajmal, M., Achite, M., & Kim, T. (2022). Comprehensive Review: Advancements in Rainfall-Runoff Modelling for Flood Mitigation. *Climate*, 10(10), 147.  
<https://doi.org/10.3390/cli10100147>

Jha, M., & Afreen, S. (2020). Flooding Urban Landscapes: Analysis using combined hydrodynamic and hydrologic modeling approaches. *Water*, 12(7), 1986.  
<https://doi.org/10.3390/w12071986>

Khaddari, A., Jari, A., Chakiri, S., El Hadi, H., Labriki, A., Hajaj, S., El Harti, A., Goumghar, L., & Abioui, M. (2023). A Comparative Analysis of Analytical Hierarchy Process and Fuzzy Logic Modeling in Flood Susceptibility Mapping in the Assaka Watershed, Morocco. *Journal of Ecological Engineering*, 24(8), 62–83. <https://doi.org/10.12911/22998993/165958>

Khoeun, C., Sok, T., Chan, R., Khe, S., Ich, I., Chan, K., & Oeurng, C. (2022). Assessing Flood Hazard Index using Analytical Hierarchy Process (AHP) and Geographical Information System (GIS) in Stung Sen River Basin. *IOP Conference Series Earth and Environmental Science*, 1091(1), 012031. <https://doi.org/10.1088/1755-1315/1091/1/012031>

Koks, E. E., Bars, D. L., Essenfelder, A., Nirandjan, S., & Sayers, P. (2022). The impacts of coastal flooding and sea level rise on critical infrastructure: a novel storyline approach. *Sustainable and Resilient Infrastructure*, 8(sup1), 237–261.  
<https://doi.org/10.1080/23789689.2022.2142741>

Kumar, V., Sharma, K., Caloiero, T., Mehta, D., & Singh, K. (2023). Comprehensive Overview of flood modeling Approaches: A review of recent advances. *Hydrology*, 10(7), 141.  
<https://doi.org/10.3390/hydrology10070141>

Kundzewicz, Z. W., Kanae, S., Seneviratne, S. I., Handmer, J., Nicholls, N., Peduzzi, P., Mechler, R., Bouwer, L. M., Arnell, N., Mach, K., Muir-Wood, R., Brakenridge, G. R., Kron, W., Benito, G., Honda, Y., Takahashi, K., & Sherstyukov, B. (2013). Flood risk and climate change: global and regional perspectives. *Hydrological Sciences Journal*, 59(1), 1–28. <https://doi.org/10.1080/02626667.2013.857411>

Kvočka, D., Falconer, R. A., & Bray, M. (2016). Flood hazard assessment for extreme flood events. *Natural Hazards*, 84(3), 1569–1599. <https://doi.org/10.1007/s11069-016-2501->

Lipovetsky, S. (2021b). Understanding the analytic hierarchy process. *Technometrics*, 63(2), 278–279. <https://doi.org/10.1080/00401706.2021.1904744>

Liu, L., Liu, Y., Wang, X., Yu, D., Liu, K., Huang, H., & Hu, G. (2015). Developing an effective 2-D urban flood inundation model for city emergency management based on cellular automata. *Natural Hazards and Earth System Sciences*, 15(3), 381–391. <https://doi.org/10.5194/nhess-15-381-2015>

Madi, M., Hafnaoui, M. A., Hachemi, A. H., Said, M. B. S., Noui, A., Chaa, A. M., Bouchahm, N., & Farhi, Y. (2020, January 30). Flood risk assessment in Saharan regions. A case study (Bechar Region, Algeria)|JBES. [https://papers.ssrn.com/sol3/papers.cfm?abstract\\_id=3569907](https://papers.ssrn.com/sol3/papers.cfm?abstract_id=3569907)

Madzik, P., & Falát, L. (2022). State-of-the-art on analytic hierarchy process in the last 40 years: Literature review based on Latent Dirichlet Allocation topic modelling. *PLoS ONE*, 17(5), e0268777. <https://doi.org/10.1371/journal.pone.0268777>

Manandhar, B., Cui, S., Wang, L., & Shrestha, S. (2023b). Urban Flood Hazard Assessment and Management Practices in South Asia: a review. *Land*, 12(3), 627. <https://doi.org/10.3390/land12030627>

Maqtan, R., Othman, F., Jaafar, W. Z. W., Sherif, M., & El-Shafie, A. (2022). A scoping review of flash floods in Malaysia: current status and the way forward. *Natural Hazards*, 114(3), 2387–2416. <https://doi.org/10.1007/s11069-022-05486-6>

Merz, B., Blöschl, G., Vorogushyn, S., Dottori, F., Aerts, J. C. J. H., Bates, P., Bertola, M., Kemter, M., Kreibich, H., Lall, U., & Macdonald, E. (2021). Causes, impacts and patterns of disastrous river floods. *Nature Reviews Earth & Environment*, 2(9), 592–609. <https://doi.org/10.1038/s43017-021-00195-3>

Mokhtari, E., Mezali, F., Abdelkebir, B., & Engel, B. (2023). Flood risk assessment using analytical hierarchy process: A case study from the Cheliff-Ghrib watershed, Algeria. *Journal of Water and Climate Change*, 14, 10.2166/wcc.2023.316.

Mondal, K. C., Saha, S., Aitch, P., & Bhandari, G. (2019). Application of Remote Sensing and GIS in Flood Vulnerability Assessment—A Case Study of Lower Ajay Basin, India. In *Disaster risk reduction* (pp. 151–166). [https://doi.org/10.1007/978-981-32-9527-8\\_10](https://doi.org/10.1007/978-981-32-9527-8_10)

Moradkhani, H., & Sorooshian, S. (2008). General Review of Rainfall-Runoff Modeling: model calibration, data assimilation, and Uncertainty Analysis. <https://escholarship.org/uc/item/42d5d6cg>

Mourato, S., Fernandez, P., Pereira, L. G., & Moreira, M. (2023). Assessing vulnerability in flood prone areas using Analytic Hierarchy Process—Group Decision Making and Geographic Information System: a case study in Portugal. *Applied Sciences*, 13(8), 4915. <https://doi.org/10.3390/app13084915>

Msatef, K., Benaabidate, L., & Bouignane, A. (2018). Hydrological and hydroclimatic regimes in the Ouergha watershed. *E3S Web of Conferences*, 37, 1–11. <https://doi.org/10.1051/e3sconf/2018370400>

Munawar, H. S., Hammad, A. W. A., & Waller, S. T. (2022). Remote Sensing Methods for Flood Prediction: A review. *Sensors*, 22(3), 960. <https://doi.org/10.3390/s22030960>

Namara, W. G., Damisse, T. A., & Tufa, F. G. (2021). Application of HEC-RAS and HEC-GeoRAS model for Flood Inundation Mapping, the case of Awash Bello Flood Plain, Upper Awash River Basin, Oromiya Regional State, Ethiopia. *Modeling Earth Systems and Environment*, 8(2), 1449–1460. <https://doi.org/10.1007/s40808-021-01166-9>

Nasiri, H., Yusof, M. J. M., & Ali, T. a. M. (2016). An overview to flood vulnerability assessment methods. *Sustainable Water Resources Management*, 2(3), 331–336. <https://doi.org/10.1007/s40899-016-0051-x>

Nastiti, K. D., An, H., Kim, Y., & Jung, K. (2018). Large-scale rainfall–runoff–inundation modeling for upper Citarum River watershed, Indonesia. *Environmental Earth Sciences*, 77(18). <https://doi.org/10.1007/s12665-018-7803-x>

Nastiti, K. D., Kim, Y., Jung, K., & An, H. (2015). The application of Rainfall-Runoff-Inundation (RRI) model for inundation case in Upper Citarum Watershed, West Java-Indonesia. *Procedia Engineering*, 125, 166–172. <https://doi.org/10.1016/j.proeng.2015.11.024>

Ongdas, N., Akiyanova, F., Karakulov, Y., Muratbayeva, A., & Zinabdin, N. (2020). Application of HEC-RAS (2D) for flood Hazard Maps generation for Yesil (Ishim) River in Kazakhstan. *Water*, 12(10), 2672. <https://doi.org/10.3390/w12102672>

Otmane, A., Gacemi, M. E., Belabid, N., & Bellabas, E. (2024). Which strategy should be adopted for the delimitation of the hydraulic public domain? The case of a watershed characterised by dam overflows and inter-basin water transfers (Boudouaou-Algeria). *Environmental Earth Sciences*, 83(20). <https://doi.org/10.1007/s12665-024-11886-7>

Ouma, Y., & Tateishi, R. (2014). Urban Flood Vulnerability and Risk mapping using Integrated Multi-Parametric AHP and GIS: Methodological Overview and case study assessment. *Water*, 6(6), 1515–1545. <https://doi.org/10.3390/w6061515>

Peng, L., Wang, Y., Yang, L., Garchagen, M., & Deng, X. (2024). A comparative analysis on flood risk assessment and management performances between Beijing and Munich. <https://www.semanticscholar.org/paper/A-comparative-analysis-on-flood-risk-assessment-and-Peng-Wang/4cd9a6ea8d3a9f03b3038ce8f92f47948540b3a4>

Phyoe, P. P., & Uchida, T. (2024b). Flood Simulation Studies with Rainfall-Runoff-Inundation (RRI) Model, Over Yangon City, Myanmar. *Proceedings of the International Association of Hydrological Sciences*, 386, 115–120. <https://doi.org/10.5194/piahs-386-115-2024>

Prieto-Amparán, J. A., Pinedo-Alvarez, A., Morales-Nieto, C. R., Valles-Aragón, M. C., Álvarez-Holguín, A., & Villarreal-Guerrero, F. (2021). A regional GIS-Assisted Multi-Criteria evaluation of Site-Suitability for the development of solar farms. *Land*, 10(2), 217. <https://doi.org/10.3390/land10020217>

Radwan, F., Alazba, A. A., & Mossad, A. (2018). Flood risk assessment and mapping using AHP in arid and semiarid regions. *Acta Geophysica*, 67(1), 215–229. <https://doi.org/10.1007/s11600-018-0233-z>

Ramsbottom, D., Wade, S., Bain, V., Hassan, M., Penning-Rowsell, E., Wilson, T., Fernandez, A., House, M., & Floyd, P. (2006). Flood risks to people: Phase 2. R&D Technical Report FD2321/IR2, Department for the Environment, Food and Rural Affairs (DEFRA), UK Environment Agency.

Rasmy, M., Sayama, T., & Koike, T. (2019). Development of water and energy Budget-based Rainfall-Runoff-Inundation model (WEB-RRI) and its verification in the Kalu and

Mundeni River Basins, Sri Lanka. *Journal of Hydrology*, 579, 124163. <https://doi.org/10.1016/j.jhydrol.2019.124163>

Rebouh, N., Tout, F., Dinar, H., Benzid, Y., & Zouak, Z. (2024). Integrating Multi-Source geospatial data and AHP for flood susceptibility mapping in Ain Smara, Constantine, Algeria. *International Journal of Disaster Risk Management*, 6(2), 245–263. <https://doi.org/10.18485/ijdrm.2024.6.2.16>

Saaty, T. L. (1980). *The Analytic Hierarchy Process* Mcgraw Hill, New York. *Agricultural Economics Review*, 70.

San, Z. M. L. T., Zin, W. W., Kawasaki, A., Acierito, R. A., & Oo, T. Z. (2020). Developing flood inundation map using RRI and SOBEK models: a case study of the Bago River Basin, Myanmar. *Journal of Disaster Research*, 15(3), 277–287. <https://doi.org/10.20965/jdr.2020.p0277>

Sayama, T., Matsumoto, K., Kuwano, Y., & Takara, K. (2019b). Application of Backpack-Mounted Mobile Mapping System and Rainfall–Runoff–Inundation Model for flash flood analysis. *Water*, 11(5), 963. <https://doi.org/10.3390/w11050963>

Sayama, T., Ozawa, G., Kawakami, T., Nabesaka, S., & Fukami, K. (2012). Rainfall–runoff–inundation analysis of the 2010 Pakistan flood in the Kabul River basin. *Hydrological Sciences Journal*, 57(2), 298–312. <https://doi.org/10.1080/02626667.2011.644245>

Sayama, T., Tatebe, Y., Iwami, Y., & Tanaka, S. (2015). Hydrologic sensitivity of flood runoff and inundation: 2011 Thailand floods in the Chao Phraya River basin. *Natural Hazards and Earth System Sciences*, 15(7), 1617–1630. <https://doi.org/10.5194/nhess-15-1617-2015>

Schwarz, I., & Kuleshov, Y. (2022). Flood vulnerability Assessment and mapping: A case study for Australia’s Hawkesbury-Nepean catchment. *Remote Sensing*, 14(19), 4894. <https://doi.org/10.3390/rs14194894>

Seejata, K., Yodying, A., Wongthadam, T., Mahavik, N., & Tantanee, S. (2018). Assessment of flood hazard areas using Analytical Hierarchy Process over the Lower Yom Basin, Sukhothai Province. *Procedia Engineering*, 212, 340–347. <https://doi.org/10.1016/j.proeng.2018.01.044>

Seejata, K., Yodying, A., Wongthadam, T., Mahavik, N., & Tantanee, S. (2018). Assessment of flood hazard areas using analytical hierarchy process over the Lower Yom Basin, Sukhothai Province. *Procedia Engineering*, 212, 340–347. <https://doi.org/10.1016/j.proeng.2018.01.044>

Sibandze, P., Kalumba, A. M., Aljaddani, A. H., Zhou, L., & Afuye, G. A. (2024). Geospatial Mapping and Meteorological Flood Risk Assessment: A Global Research Trend analysis. *Environmental Management*. <https://doi.org/10.1007/s00267-024-02059-0>

Siddayao, G., Valdez, S., & Fernandez, P. (2014). Analytic Hierarchy Process (AHP) in Spatial Modeling for Floodplain Risk Assessment. *International Journal of Machine Learning and Computing*, 4, 10.7763/IJMLC.2014.V4.453.

Siddiqui, M. J., Haider, S., Gabriel, H., & Shahzad, A. (2018). Rainfall–runoff, flood inundation and sensitivity analysis of the 2014 Pakistan flood in the Jhelum and Chenab river basin. *Hydrological Sciences Journal*, 63(13–14), 1976–1997. <https://doi.org/10.1080/02626667.2018.1546049>

Sitterson, J., Knightes, C., Parmar, R., Wolfe, K., Avant, B., & Muche, M. (2018, July 1-6). An overview of rainfall-runoff model types. *Proceedings of the 8th International Congress on Environmental Modelling and Software [iemss2018]* (Vol. 41, pp. 1-6). International Environmental Modelling and Software Society (iEMSs). [https://cfpub.epa.gov/si/si\\_public\\_record\\_report.cfm?dirEntryId=339328&Lab=NERL](https://cfpub.epa.gov/si/si_public_record_report.cfm?dirEntryId=339328&Lab=NERL)

Taherdoost, H. (2017b). Decision making using the Analytic Hierarchy Process (AHP); a step by step approach. [https://papers.ssrn.com/sol3/papers.cfm?abstract\\_id=3224206](https://papers.ssrn.com/sol3/papers.cfm?abstract_id=3224206)

Talukdar, G., Swain, J. B., & Patra, K. C. (2021). Flood inundation mapping and hazard assessment of Baitarani River basin using hydrologic and hydraulic model. *Natural Hazards*, 109(1), 389–403. <https://doi.org/10.1007/s11069-021-04841-3>

Tamiru, H., & Dinka, M. O. (2021b). Application of ANN and HEC-RAS model for flood inundation mapping in lower Baro Akobo River Basin, Ethiopia. *Journal of Hydrology Regional Studies*, 36, 100855. <https://doi.org/10.1016/j.ejrh.2021.100855>

Tariq, M. A. U. R., & van de Giesen, N. (2012). Floods and flood management in Pakistan. *Physics and Chemistry of the Earth, Parts A/B/C*, 47-48, 11-20

Tavana, M., Soltanifar, M., & Santos Arteaga, F. J. (2021). Analytical Hierarchy Process: Revolution and Evolution. *Annals of Operations Research*. <https://doi.org/10.1007/s10479-021-04432-2>

Tavana, M., Soltanifar, M., & Santos-Arteaga, F. J. (2021). Analytical hierarchy process: revolution and evolution. *Annals of Operations Research*, 326(2), 879–907. <https://doi.org/10.1007/s10479-021-04432-2>

Tempa, K. (2022). District flood vulnerability assessment using analytic hierarchy process (AHP) with historical flood events in Bhutan. *PLoS ONE*, 17(6), e0270467. <https://doi.org/10.1371/journal.pone.0270467>

Teng, J., Jakeman, A., Vaze, J., Croke, B., Dutta, D., & Kim, S. (2017b). Flood inundation modelling: A review of methods, recent advances and uncertainty analysis. *Environmental Modelling & Software*, 90, 201–216. <https://doi.org/10.1016/j.envsoft.2017.01.006>

Trivedi, A., Pyasi, S. K., & Galkate, R. (2018). A review on modeling of rainfall-runoff process. *The Pharma Innovation Journal*, 7(4), 1161-1166.

Try, S., Lee, G., Yu, W., Oeurng, C., & Jang, C. (2018). Large-Scale Flood-Inundation modeling in the Mekong River Basin. *Journal of Hydrologic Engineering*, 23(7). [https://doi.org/10.1061/\(asce\)he.1943-5584.0001664](https://doi.org/10.1061/(asce)he.1943-5584.0001664)

Try, S., Lee, G., Yu, W., Oeurng, C., & Jang, C. (2018b). Large-Scale Flood-Inundation modeling in the Mekong River Basin. *Journal of Hydrologic Engineering*, 23(7). [https://doi.org/10.1061/\(asce\)he.1943-5584.0001664](https://doi.org/10.1061/(asce)he.1943-5584.0001664)

Try, S., Tanaka, S., Tanaka, K., Sayama, T., Oeurng, C., Uk, S., Takara, K., Hu, M., & Han, D. (2020). Comparison of gridded precipitation datasets for rainfall-runoff and inundation modeling in the Mekong River Basin. *PLoS ONE*, 15(1), e0226814. <https://doi.org/10.1371/journal.pone.0226814>

Vaidya, O., & Kumar, S. (2006). Analytic Hierarchy Process: An Overview of Applications. *European Journal of Operational Research*, 169, 1-29. <https://doi.org/10.1016/j.ejor.2004.04.028>

Vignesh, K. S., Anandakumar, I., Ranjan, R., & Borah, D. (2020). Flood vulnerability assessment using an integrated approach of multi-criteria decision-making model and geospatial techniques. *Modeling Earth Systems and Environment*, 7(2), 767–781. <https://doi.org/10.1007/s40808-020-00997-2>

Vojtek, M., & Vojteková, J. (2016). Flood hazard and flood risk assessment at the local spatial scale: a case study. *Geomatics Natural Hazards and Risk*, 7(6), 1973–1992. <https://doi.org/10.1080/19475705.2016.1166874>

Waghwal, R. K., & Agnihotri, P. (2019). Flood risk assessment and resilience strategies for flood risk management: A case study of Surat City.

<https://www.semanticscholar.org/paper/Flood-risk-assessment-and-resilience-strategies-for-Waghwala-Agnihotri/57b8adb6983f36c516b3db7a49d26f78a94c8d34>

Waseem, M., Ahmad, S., Ahmad, I., Wahab, H., & Leta, M. K. (2023). Urban flood risk assessment using AHP and geospatial techniques in swat Pakistan. *SN Applied Sciences*, 5(8). <https://doi.org/10.1007/s42452-023-05445-1>

Willis, T., Wright, N., & Sleight, A. (2019). Systematic analysis of uncertainty in 2D flood inundation models. *Environmental Modelling & Software*, 122, 104520. <https://doi.org/10.1016/j.envsoft.2019.104>

World Health Organization: WHO. (2019, November 8). Floods. [https://www.who.int/health-topics/floods/#tab=tab\\_1](https://www.who.int/health-topics/floods/#tab=tab_1)

Xia, J., Falconer, R. A., Wang, Y., & Xiao, X. (2014). New criterion for the stability of a human body in floodwaters. *Journal of Hydraulic Research*, 52(1), 93-104.